



## Recent Development in Hydrodynamic and Heat Transfer Characteristics in the Three-phase Fluidized-bed System

Omar S. Mahdy , Amer A. Abdulrahman \* , Jamal M. Ali 

Chemical Engineering Dept., University of Technology-Iraq, Alsina'a street,10066 Baghdad, Iraq

\*Corresponding author Email: [Amer.A.Abdulrahman@uotechnology.edu.iq](mailto:Amer.A.Abdulrahman@uotechnology.edu.iq)

### HIGHLIGHTS

- The effect of several characteristics on hydrodynamic performance and heat transfer phenomena has been studied extensively.
- A review of most of the previous correlations for various parameters in gas-liquid-solid fluidization systems was investigated.
- CFD could be used to understand the complicated hydrodynamics of fluidization

### ARTICLE INFO

**Handling editor:** Qusay F. Alsahy

#### Keywords:

Three-phase fluidization  
Hydrodynamic  
Heat transfer  
CFD simulation

### ABSTRACT

Gas–liquid–solid fluidized beds are broadly utilized in the petrochemical, pharmaceutical, refining, food, biotechnology, and environmental industries. Due to complex phenomena, such as the particle–particle, liquid–particle, particle–bubble interactions, complex hydrodynamics, and heat transfer of three-phase (gas–liquid–solid) fluidized beds, they are incompletely understood. The ability to accurately predict the essential characteristics of the fluidized-bed system, such as hydrodynamics, individual phase mixing, and heat transfer parameters, is necessary for its successful design and operation. This paper investigates the pressure drop, minimum fluidization velocity, phase holdup, heat-transfer coefficient of a fluidized bed reactor, heat transfer studies, CFD simulation, and the effect of these parameters on the extent of fluidization. Many variables (fluid flow rate, particle density and size, fluid inlet, and bed height) affect the fluidizing quality and performance of the fluidization process. The hydrodynamics parameters, mixing of phases, and the behavior of heat transfer with various modes of fluidization were investigated to predict hydrodynamics parameters. Several publications have demonstrated the utility of (CFD) in explaining the hydrodynamics, heat, and mass transfer of fluidized beds. Principles of measurement, details of the experimental configurations, and the applied techniques by various researchers are also presented. Feng's model was statistically validated using experimental data that was both time-averaged and time-dependent. Furthermore, this model successfully predicted the instantaneous flow structures, which should provide strategies for the best design, scale-up, and operation in fluidized bed columns. The divergence between the simulated and observed values can be reduced by better understanding the fluidized bed's nature.

## 1. Introduction

Fluidized beds are widely used in various industries due to their excellent properties, including high heat and mass transfer rates between phases, temperature homogeneity, ease of handling, and rapid particle mixing. gas-liquid-solid fluidization systems ensure that the solid, liquid, and gaseous phases interact effectively and are substantially different from and more complex than two-phase systems [1]. Due to its industrial importance, three-phase fluidization has been a focus of fundamental study for the last six decades. Since then, significant progress has been made concerning appreciating the gas-liquid-solid fluidization phenomenon. A fluidized bed system's efficient design and operation require accurately estimating the essential system properties [2]. The three-phase fluidization is considered a process in which a bed of solid particles is suspended in gas and liquid media due to the net drag force of the flow in opposition to the net gravitational force (or buoyancy force) on the particles. Such an operation creates a significant interaction between the gas-liquid media and the solid particles, providing essential advantages in chemical, physical, and biochemical processing [3]. For a three-phase fluidization system, bubbles are formed as a gas phase that provides an efficient interaction with both liquid and solid phases; due to the upward flow of

Bubbles and liquid, the solid particles will suspend or fluidize and behave as a liquid phase. The most important characteristics for the broad application of three-phase fluidization are the high heat transfer rates. It refers to the efficient mixing of

Hydrodynamic generated by bubble-liquid movement and the interaction of this movement with solid particles. A better understanding of the effects of hydrodynamic structures on heat transfer is an essential task to improve the design and operation of three-phase reactors with the fluidized bed [4]. The minimum fluidization velocity, pressure drop, and phase holdup are all essential characteristics in the process of a fluidized bed reactor. Several researchers have studied the minimum fluidization conditions and phase holdup to find empirical correlations for the onset of particle fluidization. Computational fluid dynamics (CFD) has been increasingly typical as a method for simulating multi-phase flow in recent years. It offers a faster and easier way of accurately predicting hydrodynamic characteristics without the need for costly and time-consuming experiments.

Furthermore, the CFD method is reliable for tests involving high pressures and temperatures in dangerous operating conditions. CFD simulations can be divided into Eulerian–Eulerian and Eulerian-Lagrangian [5]. The state of gas-liquid-solid fluidization depends significantly on the bed geometry, gas-liquid input methods, and the availability of retaining grids or internals. A fluidized tapered bed, spouted bed, semi-fluidized bed, and spouted bed draft tube are examples of this design and activity [6].

## 2. Criteria of the Phenomenon of Fluidization

The ability to accurately predict the system's fundamental properties is essential to the effective design and operation of a gas-liquid-solid fluidized bed system. Specific aspects must be expected and quantified to build a three-phase fluidized bed chemical reactor [7]. Table 1 lists some of the principal terms used to explain the fluidization process.

**Table 1:** Descriptions of specific terms related to three-phase fluidization

Term	symbol	Signi fication
Pressure drop throughout the bed	$\Delta P$	Measures drag as well as buoyancy and phase holdups. [8].
Minimum fluidization velocity	$U_{mf}$	The bed fluidizes at a minimum superficial velocity. The particles are primarily fluidized by liquid [9].
Bed expansion ratio	$\beta_{er}$	Measure the extent of fluidization of the bed[ 10].
Gas holdup	$\epsilon_g$	Measure the Gas occupied fractional volume[ 11].
Liquid holdup	$\epsilon_L$	Measures the fraction of the bed that is occupied by the liquid phase [12].
Solids holdup	$\epsilon_s$	Measure the volume of fractions occupied by the solids[13].
Porosity	$\epsilon$	Measures the volume that both the liquid and gas occupy [ 14].
Bubble rise velocity	$U_b$	A bubble's actual velocity as it rises through the bed[2].
Bed Fluctuation Ratio	$r$	The highest and lowest levels ratio is occupied by the top of the bed[ 15].
Phase velocity	$U$	Individual phase velocities in a fluidized bed [ 12].

## 3. Variables Influence the Fluidization Quality

Many variables affect the fluidizing quality and performance of the gas-liquid-solid fluidization process, as shown in Figure 1. This text will discuss these factors, including particle-size variations that play a crucial role in enhancing fluidization. Mainly, a wide variety of particle sizes is preferred rather than standardized measures for adequate mixing [16]. Fluidization of larger particles requires a large amount of pressure force. As a result, minimum liquid fluidization increases as a particle size increases [14]. The fluid flow rate will be high for the suspension of solids in fluid, but more growth in the channeling of fluid flow rate occurs [17]. At a steady liquid flow rate, the pressure drop of the column decreases as the air flow rate increases. The bed is initially fluidized by liquid and remains that way at this point [18].

Fluid distribution in the bed is necessary for the fluidized bed design. It is challenging to obtain successful fluidization when the bed height is higher [19]. Increases in liquid and gas velocities increase the expansion ratio, decreasing as the particle size and static bed height increase. Still, the initial static bed height does not affect the minimum fluidization velocity. The closer the particle density to gas and liquid, the easier the fluidization can be maintained [20]. The extraction efficiency also increases with temperature rise to a limited range [21], and the position of the heater should be sufficient to achieve desired fluid flow at the desired temperature [22]. The minimum fluidization velocity was inversely proportional to the temperature and directly proportional to the mean particle size. For all sizes of bed particles, the pressure drop was discovered to increase with bed temperature [23].

## 4. Hydrodynamic on Gas-Liquid-Solid Fluidization

For more than 60 years, hydrodynamic characteristics on three-phase fluidized beds have been under academic and commercial investigation; the literature today abounds with studies on this topic. This resulted in the publication of a wide variety of experimental data and theoretical principles intended to understand better these reactors' behavior in operation [24]. In addition, many researchers have investigated the hydrodynamic of three-phase fluidized beds experimentally. The detailed investigations based on experiments carried out in columns of the small scale are described in Table 2. This table also includes

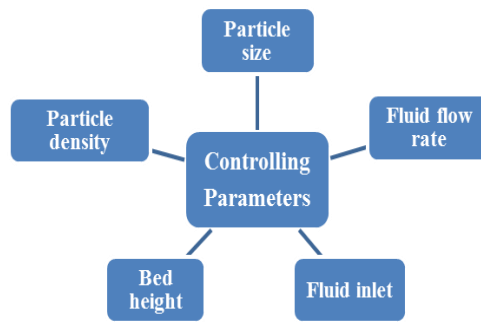


Figure 1: Factors affecting fluidized bed performance

brief details about the studied techniques and systems which used the glass beads as the solid phase in this experiment. The hydrodynamics, mixing of individual phases and mass and heat transfer properties all play a role in designing and operating a gas-liquid-solid fluidized bed system. The most critical hydrodynamic parameters are the minimum fluidization velocity, pressure drop, phase hold up, and bed expansion. Depending on particles' density and volume fraction, a three-phase reactor can be divided into two types: A Fluidized-bed reactor and a slurry bubble-column one.

However, as indicated in Table 3, some experiments have used solid-phase types other than glass beds. Some of these hydrodynamic investigations of the three-phase fluidized bed are listed in Table 3.

Solids have a substantially higher density than the fluid in fluidized bed reactors, where the volume fraction of solids is between 0.2 and 0.6, and the particle size is more than 150  $\mu\text{m}$ . In a slurry bubble column reactor, the density of the solids is slightly higher than that of the fluid; the volume fraction of the particles is less than 0.15, and the particle size ranges from 5-150  $\mu\text{m}$  [13].

According to the literature, most of the experiments were conducted in a three-phase fluidized bed reactor using glass beads as the solid phase. However, only a few experimental studies involving gas-liquid-solid fluidization used alternative types of solid phases, such as (sand, wood, polystyrene, acetate, alumina, activated carbon, etc. Glass beads are used because of their high strength, enhanced processing, chemical stability, low oil absorption, minimal thermal expansion, good flowability, and colorless glass. Knesebeck et al. [35] investigated the particle size distribution along with the bed height when fluidized solid particles with a wide size distribution. The concentration profiles of particles of each size class were determined at various liquid and gas velocities by obtaining suspension samples at different axial and radial locations. The flow of gas bubbles and the effect of wake-up bubbles appear to be the determinants of gas velocity. As a result, increasing the gas velocity improves particle carryover and mixing. These phenomena explain smaller particles that separate from the dense bed and concentrate in the top lean zone. Simultaneously, mixing in the dense bed improves, and axial concentration profiles of particles of various size groups within the dense bed appear to be more uniform. Jena et al. [29] conducted the hydrodynamic analysis of the three-phase fluidized bed. They showed that with an increase in particle size at constant gas velocity, the minimum liquid fluidization velocity ( $U_{Lmf}$ ) increases but decreases with an increase in gas velocity at constant liquid velocity. The expansion ratio increases with increased liquid and gas flow rate but decreases with particle size and static bed height. Sivalingam et al. [31] studied the significant role of hydrodynamics in the economic designing and operation of a three-phase fluidized bed. Different characteristics such as pressure drop, porosity, gas, and liquid holdups were investigated about fluid rates. As the flow rate rise, the gas holds up, and bed porosity increases. When comparing the effects of gas and liquid velocities on hydrodynamic characteristics, it is evident that the influence of the gas velocity on the various parameters is greater than the influence of the liquid velocity. Therefore, the gas flow rate is dominant in the fluidized bed design. Sulaymon et al. [38] investigated the three-phase hydrodynamic characteristics of non-Newtonian liquid-gas-solid fluidized beds. Depending on bubble column operating conditions and physical properties of liquids, the phenomenon of liquid circulation for highly viscous Newtonian and non-Newtonian liquids can be observed. A gas holdup in three-phase fluidized beds increases with increasing superficial gas velocity for all particle sizes studied. With the increase in particle size at constant gas velocity, the minimum velocity of liquid fluidization increases. Pare [7] studied the hydrodynamic characteristics of a low-density particle in a three-phase (gas-liquid-solid) fluidized bed using the liquid phase as water while the gas phase as air. The bed pressure drops, minimum fluidization velocity and bed expansion ratios, and the hydrodynamic characteristics evaluated, were included. These parameters' dependence on particle diameter, initial static bed height, liquid velocity, and gas velocity has been investigated. Results show that the bed pressure drops with gas velocity, and minimum fluidization velocity decrease but increases with particle size. The bed expansion ratio increases with increasing liquid values but decreases with  $d_p$  and initial static bed height [8]. Sinha et al. [13] studied the hydrodynamic characteristics of three-phase for low-density particles (solid wood). Results show that the minimum fluidization velocity and bed pressure drop increase with a particle size but decrease with a gas velocity. The bed expansion ratio decreases with particle size and an initial static bed height but increases with liquid values. Nan et al. [41] investigated the Inverse Gas-Liquid-Solid Circulating Fluidized Bed (IGLSCFB) as a complement to the Inverse Liquid-Solid Circulating Fluidized Bed (ILSCFB). It is described the operation window for solids downflow and gas up the flow. It was also discovered that the change in solids holdup as a function of operating conditions is highly similar to the ILSCFB.

Gas affects solids holdup, but it is not extreme. Alward et al. [43] used a new type of rotating three-phase fluidized bed reactor (spiral three-phase fluidized bed reactor (TPFB-S)) to remove engine oil (both virgin and waste form) from synthetic wastewater was examined. The materials were characterized using SEM images and FTIR analyses, which revealed that RC

leaves have high biosorption in terms of surface shape and active groups—changing the experimental variables such as particle size, liquid and gas flow rate significantly impacted the biosorption performance of RC leaves for oil emulsion in the TPFB-S reactor. Using the natural and activated forms of *Ricinus communis* RC, at 150–300  $\mu$ m particle size, 3.5 L/min liquid flow rate, and 1 L/min air flow rate, the maximum removal efficiency for virgin and waste oil was 91 and 98 %, respectively. The results showed that the spiral unit could generate upward water flow, reducing the load of the water treatment in conventional TPFB and increasing the removal effectiveness of pure oil emulsion by around 23 and 17 % for natural and activated RC leaves, respectively.

#### 4.1 Minimum Fluidization Velocity ( $U_{Lmf}$ )

The most common hydrodynamic parameter of primary importance in the design of a fluidized three-phase bed is the minimum liquid velocity of fluidization ( $U_{Lmf}$ ). It is usually referred to as the minimum fluidization liquid velocity ( $U_{Lmf}$ ) at the specified superficial gas velocity for the co-current up-flow gas-liquid-solid fluidized beds since the continuous liquid phase is the primary fluidization medium [44]. When a fluid moves up through the interstices of a solid bed without the slightest disturbance to the solids, the bed is considered a fixed bed. For a further increase in fluid velocity, the whole bed of solids becomes suspended and behaves as if its weight becomes counterbalanced by the buoyancy force. All particles are

entirely suspended in the fluid at this point [45]. Visual observation and hydrostatic pressure drop analysis of the multi-phase flow are frequently used to estimate  $U_{Lmf}$ . Additionally,  $U_{Lmf}^{L-s}$  is calculated by mathematical, fractal, disorder, wavelet, and neural network analyses [32]. The Ergun equation (Ergun [46]) is the generally known model for determining a fluid's minimum fluidization velocity to fluidize the particle [47].

$$(1 - \varepsilon_{mf})(\rho_s - \rho_f)g = 150 \frac{(1 - \varepsilon_{mf})^2 \mu u_{mf}}{\varepsilon_{mf}^3 \phi_s d_p^2} + 1.75 \frac{(1 - \varepsilon_{mf}) \rho_f u_{mf}^2}{\varepsilon_{mf}^3 \phi_s d_p} \quad (1)$$

The Ergun equation consists of viscous and kinetic energy (1st and 2nd part of Equation (1)). The fluidization behavior in the Ergun equation was primarily governed by the kinetic energy concept in the case of larger particles. It is also necessary to reduce the Ergun equation to the following one.

$$U_{mf}^2 = \frac{\phi_s d_p (\rho_s - \rho_f)}{1.75 \rho_f} g \varepsilon_{mf}^3 \quad (2)$$

Begovich and Watson [3] reported the correlation given the following equation for a three-phase fluidized bed containing large or dense particles. It can be used to predict the minimum fluidization velocity for monocomponent systems.

$$\frac{U_{Lmf}}{U_{Lmf}^{L-s}} = 1 - U_g^{0.436} \mu_L^{0.27} d_p^{0.598} (\rho_s - \rho_L)^{-0.305} \quad (3)$$

Many articles have been reported on the minimum velocity of fluidized beds in three phases (Begovich and Watson, [3]; Fortin, [48]; Costa et al., [49]; Song et al., [50]; Nacef et al., [51]; Zhang et al., [52]; Ramesh et al., [53]; Ruiz et al., [54]; Sivasubramanian et al. [34]; Jena et al., [2] and Li et al., [32]). Many studies of the minimum fluidization velocity in three-phase fluidized beds are limited to air-water glass bead systems whose particle density exceeds that of the liquid by a factor of 2 to 3 [25]. Sivasubramanian et al. [34] Investigated the  $U_{Lmf}$  showed a growing pattern with an increase in the particle diameter. As the liquid phase was studied, the effect of superficial gas velocity,  $U_g$  on  $U_{Lmf}$  (minimum fluidization liquid velocity) was examined. In addition, the effect of superficial liquid velocity,  $U_l$ , on  $U_{gmf}$  (minimum fluidization gas velocity) for water, glycerol, and carboxymethyl cellulose (CMC), was studied.  $U_{Lmf}$  decreased with an increase in  $U_g$ , and an increase in  $U_l$  also reduced the  $U_{gmf}$ .  $U_{Lmf}$  decreased with the increased viscosity (concentration) of glycerol and CMC. Correlations to  $U_{Lmf}$ 's prediction of Newtonian and non-Newtonian models are suggested. Venkatachalam et al. [39] reported that the minimum fluidization velocity decreases when the gas velocity, particle diameter, and liquid viscosity increase. The minimum fluidization velocity is reduced as the fluid consistency index increases. With increasing surface tension, the minimum fluidization velocity decreased, while for the liquid holdup, surface tension increased. Correlations were developed for minimum fluidization velocity and riser liquid holdup based on the properties of liquid and solid phases and was observed to agree with the experimental results. The design of commercial reactors could confidently use these correlations. Li et al. [32] have been experimentally investigated that  $U_{Lmf}$  cannot be calculated in 3-5 mm MFBs. Both data analyses of the pressure drop and Hurst exponent can be used to verify  $U_{Lmf}$  for 8-10 mm MFBs with low surface gas velocity. However,  $U_{Lmf}$  could not be obtained at high superficial gas velocity since the turning point where the flow regime transformed from packed to fluidize disappeared, leaving the bed in a half-fluidized state. For the effective working of gas-liquid-solid fluidized beds, accurate prediction of a minimum condition of liquid fluidization is essential, especially when a particle or liquid properties are involved. Previous minimum fluidization velocity correlations in gas-liquid-solid systems are listed in Table 4.

Begovich's correlation with a total of 125 data points showed a correlation coefficient of 0.93 and an F-value of 179. This correlation's dimensional is statistically less satisfying, but it behaves correctly when gas velocity approaches zero. Costa's correlation has a high degree of accuracy, with deviations never exceeding 10%. In the range of variables tested, this equation demonstrated a better prediction. Ramesh's data, which consisted of 209 experimental measurements, was utilized (184 data

points from three-phase systems and 25 data points from two-phase systems). RMS errors were 9.0 %, with a maximum variation of 20% for both two-phase and three-phase systems, showing a better representation of the minimum fluidization velocity data for both two-phase and three-phase systems using RSM (response surface methodology). Using 115 literature data from six different papers on minimum fluidization velocity, a new correlation for the computation of minimum fluidization velocity in two-phase ( $V_{g=0}$ ) and three-phase systems is also established, with errors proven to be within 14%. For Newtonian systems, Sivasubramanian's correlations were found with ( $R^2=0.95$ ). With an average RMS error of 16 %, Sivasubramanian's proposed equations accurately predicted the experimental data for Newtonian systems. A total of 252 practical points from Li's data were used. The Li's correlation average deviation value is 6.36%. The empirical correlation value agrees well with the results of the experiments.

**Table 2:** Hydrodynamic gas-liquid-solid fluidization studies with glass beads as solid phase

Fluidizing medium		Solid	$\rho_s$ kg/m <sup>3</sup>	$d_p$ mm	$D_c$ m	$H_c$ m	UL m/s	$U_g$ m/s	Remarks of study	Ref.
Liquid	Gas									
Glycerol solution, Silicone oil, Water.	Air	Glass beads	2230	3.2	0.127	3	0.0-0.002	0.0-0.00604	As $U_g$ increases, $U_{mf}$ decreases. With increasing superficial gas velocity, the voidage at minimum fluidization, $\epsilon_{mf}$ , tends to reduce initially to a minimum and gradually increase.	Lee et al. [25]
				6.0						
				3.3						
				5.5						
Aqueous Na <sub>2</sub> HPO <sub>4</sub> sol.	Air	Glass beads	2471	3	0.1	2	0.000	0.010 - 7-0.052	The bed was always in the coalesced bubble flow regime during the whole range of operating conditions.	Briens et al.[26]
				2.1						
Water-alcohol sol.	Air	Glass beads	2500	1.2, 5	0.152	2.75	0.0 - 0.07	0.011 - 0.170	Surface-active agents increased gas holdups in a bubble column by an average of 41%.	Dargar et al.[27]
Water CMCS sol.	Air	Glass beads,	2460	1.25, 1.45	0.15	4.35	0.03 - 0.09	0.01 - 0.05	The value of local gas holdup has been highest in the center and lowest along the wall. The local gas holdups in non-Newtonian fluids are slightly smaller than in water.	Cao et al. [28]
Water	Air	Glass beads	2216	2.18	0.1	2	0.0-0.16	0.0-0.12	At a constant gas velocity, gas hold-up reduces at the low liquid rate and remains constant as the liquid velocity increases. With the increase in particle size, the gas hold-up increases.	Jena et al. [29]
				2.58						
				3.05						
				4.05						
Water	Air	Glass beads	2490	0.62-0.98	0.102	0.962	0.0-0.018	0.0-0.007	The upward flow of bubbles in a gas-liquid-solid conical fluidized bed creates more agitation on packed particles in the upper section of the column, loosening particles and reducing particle-particle interaction.	Zhou et al. [30]
Water	Air	Glass beads	2500	4.38, 1.854	0.054	1.6	0.0-0.3	0.0-2.5	The gas flow rate is significant in the fluidized bed design. The system is primarily dependent on solid-liquid interaction.	Sivalingam et al. [31]

**Table : 2 Continued**

Fluidizing medium		Solid	ps kg/m3	dp mm	Dc m	Hc m	UL m/s	Ug m/s	Remarks of study	Ref.
Liquid	Gas									
Water	Air	Glass beads	2216 2253 2270	2.18, 305, 4.05	0.1	1.88	0- 0.148 6	0 - 0.12	At the same operating conditions, a gas holdup in the semi-fluidized bed was 40% greater than in the fluidized bed for some instances.	Jena et al. [2]
Water, glycerol-sol., Water with surfactant	Air	Glass beads	2500	0.104-0.946	0.03-0.005 0.008-0.01	0.50 0.1	0.0- 0.025	0.0-0.012	The fluidization of solid particles is supported by the complex bubble-growing behavior caused by the interaction of characteristics of the gas-liquid mixture and bed walls, which leads to a reduction in ULmf.	Li et al. [32]
Electrolyte Sol.	Nitrogen	Glass balls	2500	4.248-5.613	0.0673	1.5	0- 0.35	0-0.1	Increases in gas velocity, pitch, sphere diameter, and particle diameter were observed to increase gas holdup. The effects of gas velocity, pitch, and rod diameter on liquid holdup were insignificant.	Kumar et al.[33]

**Table 3:** Hydrodynamic gas-liquid-solid fluidization studies with other than glass bed as the solid phase

Remarks of study	Fluidizing medium	Solid	ps kg/m3	dp mm	Dc m	Hc m	UL m/s	Ug m/s	Remarks of study	Ref.
Glycerol solution, Silicone oil, Water.	Air	Alumina (in silicone oil) Polymer blend Polystyrene	1881 1280 102	3.2 3.3 5.5	0.127	3	0.0- 0.00279	0.0- 0.00604	Because local agitation by the gas bubbles leads to s to bed compaction around the minimum liquid fluidization velocity, Emf is smaller for three-phase systems than for corresponding two-phase (liquid-solid) fluidized beds.	Lee et al. [25]
Water, CMC sol, glycerol sol.	Air	Polypropylene polyethylene	830 940	4,6,8 4,6,8	0.1	1.8	0.0-0.02	0.0- 0.00188	With an increase in viscosity (concentration), both Ulmf and Ugmf decreased in Newtonian (glycerol) and non-Newtonian (CMC) systems. For the systems tested, Ugmf decreased as Ul increased.	Sivasubramania et al. [34]
Water	Air	Alumina	1810	0.131 0.155	0.06	2.98	0.0- 0.00088 7	0.0-0.004	Smaller particles detach from the dense bed and condense in the top lean zone. At the same time, mixing in the dense bed improves, resulting in more uniform axial concentration profiles of particles of various sizes inside the thick bed.	Knesebeck et al. [35]
Water	Air	TiO2 nanoparticles	4260	10 nm	0.2	1.2	0.4	0.01-0.03	With increasing superficial gas velocity, the local averaged axial liquid velocity and local averaged gas holdup increased, decreasing with increasing TiO2 nanoparticles loading and the axial distance from the bottom of the bubble column.	Feng et al. [36]
Aqueous Na2HPO4 sol.	Air	Polypropylene	1290	3 2.1	0.1	2	0.0007- 0.056	0.010 - 0.052	Low-density polypropylene particles were used in the three-phase bed. With a superficial gas velocity of 0.023 m/s, Ucd was essentially independent of it.	Briens et al.[26]
Water	Air	Ceramic raschig ring	1670	5.6 3.3	0.1	2	0.0-0.18	0.0- 0.06369	The Ulmf increased as particle size increased, decreased as gas velocity increased, and is unaffected by bed mass.	Aditya et al. [37]

Table 3:Continued

Remarks of study	Fluidizing medium	Solid	ps kg/m <sup>3</sup>	dp mm	Dc m	Hc m	UL m/s	Ug m/s	Remarks of study	Ref.
Water CMC sol.	Air	styrene resin	1264	1.45	0.15	4.35	0.03 - 0.09	0.01 - 0.05	When $\rho_s/\rho_l \approx 1$ , the solid local holdup increased so little and stayed nearly constant at $r_p/R = 0-0.6$ for the polymer particle.	Cao et al. [28]
Water	Air	Activated carbon	1317	0.64	0.10 2	0.962	0.0- 0.018	0.0- 0.007	The conical bed's minimum fluidization velocity is also higher than the cylindrical bed's. A decrease in particle drag forces accompanies the drop in fluidizing velocity with bed height in a conical bed.	Zhou et al. [30]
CMC sol.	Air	Activated carbon,	770	0.75, 0.25	0.10	2	0.0- 0.1	0.0-1.6	More complex hydrodynamic behavior emerges when the superficial gas velocity exceeds 0.12 m/s, resulting in the transition from bubbly to churn-turbulent flow regime.	Abbas et al. [38]
Water, glycerol, and n-Butanol sol. CMC sol.	Air	Sphere- Porcelain, Bear saddles Rasching rings	2478, 2480, 2213- 2456	1-10 6.5-11.5  3.51,13.6	0.15, 0.03	1.7	0.0- 0.08	0.00014 2 - 0.0674	When the fluid constancy index of non-Newtonian liquids increases, the liquid holdup decreases. When the viscosity of Newtonian fluids was increased, a similar tendency was found. The minimum fluidization velocity decreased as surface tension increased, yet the liquid holdup velocity increased as surface tension increased.	Venkatachalam et al. [39]
Water, kerosene sol.	-	Spherical plastic, PVC particles	1044 1115 1025	8, 15, 3.34	0.106	2	0.0- 0.042		The holdup of the continuous phase increases as the velocity of the continuous phase and particle diameter increases, while it decreases as the velocity of the dispersed phase increases.	Thamer et al. [40]
Water	Air	Wood	1142, 1111, 1111	3.7, 6.2, 8.7	0.1	1.24	0.0- 0.06	0.0-0.008	The minimum fluidization velocity ( $U_{Lmf}$ ) is a function of particle size rather than initial static bed height, and it decreases with gas velocity while increasing with particle size.	Sinha et al. [13]
Water, glycerol-sol., Water with surfactant	Air	Amberlite IR120 Na Al <sub>2</sub> O <sub>3</sub>	1350 3800	0.615 0.276	0.00 3- 0.00 8- 0.01	0.05 0.1	0.0- 0.025	0.0- 0.012	Larger gas bubbles enhance $U_{Lmf}$ decrease. Both an increase in liquid viscosity and a reduction of liquid surface tension reduce the size of gas bubbles, which works against the decrease in $U_{Lmf}$ . It differs from the macroscale system in several ways.	Li et al. [32]
Water	Air	expanded polystyrene (EPS)	28 -1020	0.8-1.2	0.07 6	5.4	0.0052 -0.417	0.0- 0.00175	Gas holdup increases with superficial gas but is unaffected by the solid's circulation rate. Solids holdup increases as the solids circulating rate and superficial gas velocity increase but decreases as the superficial liquid velocity increases.	Nan et al. [41]
Wastewater	Air	granular zeolite	80	19-25, 13-19, 6-13, 3-6, 1.6-3	0.2	1	0.07- 0.14	0-0.95	Organic matter removal in BOD and COD was greater than 90%, although it was done mostly through filtration units due to particle matter retention.	Calvachi et al. [42]
Fresh and waste oil	Air	Ricinus particles	796	0.15-0.3 and 0.3-0.6	0.125	13.5	0.0004- 0.0012	0.0- 0.00136	The removal efficiency of pure oil emulsion from aqueous solution by natural and activated forms of adsorbent was increased by around 23% and 17%, respectively, in a spiral three-phase fluidized bed reactor compared to a traditional fluidized bed.	Alward et al. [43]

**Table 4:** Correlations on minimum fluidization velocity.

Correlation	Ref.
$\frac{U_{Lmf}}{U_{Lmf}^{L.s}} = 1 - U_g^{0.436} \mu_L^{0.227} d_p^{0.598} (\rho_s - \rho_L)^{-0.305}$	Begovich et al. [3]
$U_{Lmf} = 0.427 U_g^{-0.198} d_p^{1.539} (\rho_s - \rho_L)^{0.775}$	Fortin [48]
$U_{Lmf} = 0.0006969 U_g^{-0.328} \mu_L^{-0.355} d_c^{0.042} (\phi_s d_p)^{1.086} (\rho_s - \rho_L)^{0.865}$	Costa et al. [49]
$\frac{U_{Lmf}}{U_{Lmf}^{L.s}} = 1 - 376 U_g^{0.327} \mu_L^{0.227} d_p^{0.213} (\rho_s - \rho_L)^{-0.423}$	Song et al. [50]
$\frac{U_{Lmf}}{U_{Lmf}^{L.s}} = \exp[-13.8 Fr_g^{0.35} (\rho_s - \rho_L)^{-0.38}]$	Nacef et al. [51]
$Re_{Lmf} = [33.7^2 + 0.0406 Ar (1 - \epsilon_{gmf})^{0.5} - 33.7]$	Zhang et al. [52]
$Re_{Lmf} = 0.6(1 + Fr_g)^{-1.85} Ar^{0.3} Mo^{-0.09} \phi_s^{0.04}$	Ramesh et al. [53]
$\frac{U_{Lmf}}{U_{Lmf}^{L.s}} = 1 - 0.5 U_g^{0.075} - (\epsilon_{mf} \beta_{gmf}) \phi_s^{-0.93}$	Ruiz et al. [54]
$Re_{Lmf} = [7.033 \times 10^{-2} \times Ar_m^{0.3} Ar_m^{0.113} Re_g^{0.781}]$	Sivasubramanian et al. [34]
$\frac{U_{Lmf}}{U_{Lmf}^{L.s}} = 0.465 U_g^{-0.268} \mu_L^{-0.216} d_p^{-0.08} (\rho_s - \rho_L)^{-0.218}$	Jena et al.[2]
$Re_{Lmf} = 0.103 Ar^{2.7933} Fr_g^{-0.1984} \left(\frac{D_h}{d_p}\right)^{-0.38} \left(\frac{H_s}{D_h}\right)^{0.8938} \left(\frac{\sigma_l}{\sigma_w}\right)^{-0.3988}$	Li et al.[32]

### 4.2 Pressure Drop ( $\Delta p$ ).

Another important parameter that must be considered in explaining the hydrodynamic behavior of a three-phase fluidization bed is the pressure drop through the bed. It contr

ols the formation of the channel and slug, thus mixing the bed material with the fluid[45]. A different behavior was observed in the three-phase fluidized bed when the liquid velocity was increased at a constant gas velocity. Initially, the fixed bed was in a very densely packed state. As the velocity of the liquid rose, the bed was momentarily fluidized, a narrowly achieved packed state where the decreased drop in frictional pressure was not strong enough to hold the bed fluidized. Therefore, higher liquid velocities were needed for permanent fluidization of the bed [55]. Furthermore, studies have established that if a bed is densely packed, the pressure drop overshoots the fluidization pressure until the particles separate and fluidize, as shown in Figure 2 (state A). Upon fluidization of the particles, the fluidization curve fits the same path for fluidization and de-fluidization, as shown in Figure 2 in (state B)[56].

The overall axial pressure gradient (static pressure gradient) at any cross-section of the column in a stable state reflects the total bed weight of the three phases per unit volume, as computed by

$$d_p/d_z = g(\rho_g \epsilon_g + \rho_L \epsilon_L + \rho_s \epsilon_s) \tag{4}$$

Equation 4 can be realized from Wallis's one-dimensional multi-phase flow model, suggesting that the frictional drag on the column wall with the gas and liquid flow acceleration can be ignored.

The right-hand side term  $\epsilon_g \rho_g$  in equation 4 is generally negligibly due to its small value compared to the other words.

### 4.3 Phase Holdups ( $\epsilon$ )

In a multi-phase system, the phase holdup is described as the volume fraction occupied by the system phase considered. The solids hold up is almost distributed evenly around the column height in a fluidized bed column [58]. Thus, the relationship between phase holdups is summarized in the following equation:

$$\epsilon_s + \epsilon_L + \epsilon_g = 1 \tag{5}$$

The average holdup of solids can be measured using:

$$\epsilon_s = M_s / \rho_s A_c H_e \tag{6}$$

Where  $A_c$  is the column's cross-sectional area;  $H_e$  is the dispersion height;  $M_s$  is the solid mass of the column. Equations (4) to (6) could be used to calculate individual holdups.

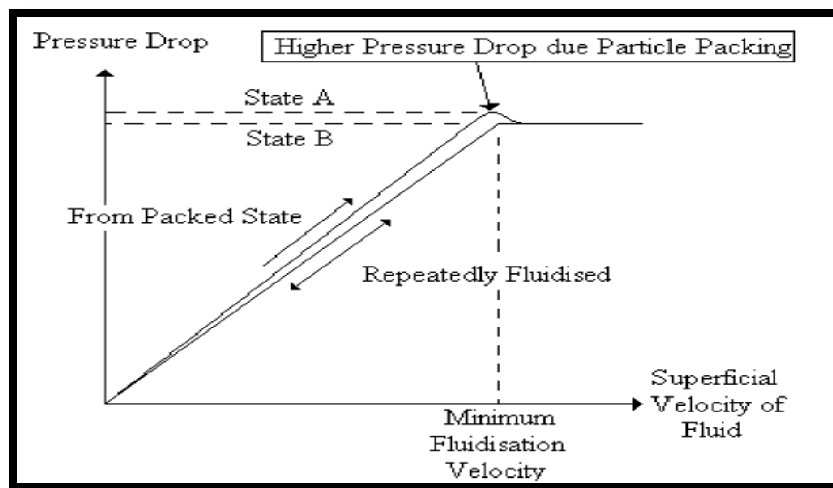


Figure 2: Dynamic pressure variations function of superficial fluid velocity [56].

#### 4.3.1 Gas holdup ( $\epsilon_g$ )

One of the most important properties to consider is the gas holdup when evaluating the efficiency of a fluidized three-phase bed. Estimating the gas holdup in chemical processes is necessary when the rate-limiting step is gas-liquid mass transfer, directly related to the mass transfer [59]. Gas holdup  $\epsilon_g$  can also be defined as the ratio of gas volume to a total volume of gas and liquid/solid mixture in a finite column length. It is necessary to distinguish the relationship between gas-liquid slip velocity and gas holdup to predict the gas holdup values [60]. These parameters are more or less affected by the hydrodynamic properties, such as the gas distributor design[61], Column diameter, height, and properties of liquid[62]. The design, optimization, and scale-up of the bubble column reactor are a focus issue to optimize specific operational parameters to improve the gas holdup and phase interface field in the column. A more direct strategy of measuring  $\epsilon_g$  is to separate an agent portion of the test section simultaneously by shutting two fast closing valves and measuring the division of the separated volume involved by the gas (Epstein, 1981). Other promising methods for calculating the local gas holdup are the system of electro-conductivity stated by Bhatia et al.[63], Ostergaard[64], Begovich et al.[3], and Yu et al.[65] radioactive tracer techniques[66]. Table 5 lists some of the more well-known gas holdup correlations with bed expansion and the authors who presented the research.

Based on a total of 913 points, Begovich's correlation had a coefficient of 0.93 and an F-value of 1793. Over % of the data fits within 30% of the calculated values, according to Gorowara's empirical correlation, this is based on over 300 experimental data points. A standard deviation of 0.037 is obtained. For Ramesh's correlation, the RMS errors were 13% (772 data for  $Re_L \leq 100$ ) and an overall error of 11.5 %, with a maximum variance of  $\pm 22$  % for the complete data set. The proposed correlation for calculating gas-phase holdup shows significant improvement and simplification over the current correlations. Jena's data were modeled using a power-law equation that passed through the origin (zero gas holdups at zero gas flow). For the ( $362.3 \leq Re_L \leq 905.7477$ ) and ( $217.3795 \leq Re_g \leq 1086.897$ ) ranges (with a standard deviation of 0.00785 and a correlation factor of 0.9821). Jena's correlation has been developed for estimating the gas holdup. The results of the developed correlation were compared to those of the experiments and those of Safoniuk's correlation. The developed correlation was valid over various operational conditions, indicating its validity. The average deviation of Kumar's correlation from regression analysis was 0.0829, with a standard deviation of 0.136 in a laboratory-scale gas-liquid-TiO<sub>2</sub> nanoparticles three-phase fluidized bed column. Feng et al. [33] used a laser Doppler anemometer (LDA) and conductivity probes to examine local hydrodynamic performance such as gas holdup and liquid velocity. The influence of various operating parameters on local gas holdup and liquid velocity has been thoroughly investigated. The local average axial liquid velocity and local average gas holdup increased with superficial gas velocity. Still, they dropped with increasing TiO<sub>2</sub> nanoparticle loading and axial distance from the bottom of the bubble column. Dargar et al. [27] studied the effects of surface-active chemicals and operating conditions on the hydrodynamic characteristics of multi-phase reactors. The addition of surface-active substances increased gas holdups by 41% on average in a bubble column. Surface-active agents increased gas holdups by an average of 37 % in a three-phase fluidized bed, while liquid and solids holdups were reduced by an average of 6.2 and 4.5 %, respectively. Jena et al.[29] Investigated for varying particle sizes and static bed heights, the influence of liquid velocity on phase hold-up, minimum liquid fluidization velocity, pressure drop, and expansion ratio. The expansion ratio of a fluidized bed was investigated in an experimental study using statistical design, and a correlation for the gas hold-up was produced. The correlation shows that gas hold-up is strongly influenced by modified gas Reynolds number but unaffected by liquid Reynolds number.

**Table 5:** Gas holdup correlations in fluidized gas-liquid-solid beds

Correlation	Ref.
$\epsilon_g = 0.048U_g^{0.720}d_p^{0.168}D_c^{0.125}$	Begovich and Watson [3]
$\epsilon_g = 0.066[U_L/(U_L + U_s)]^{-0.424}$	Catros et al. [67]
$\epsilon_g = 0.048Fr_{g,dh}^{0.315}Fr_{L,dh}^{-0.098}M_o^{0.02}(1 + 34.09 d_p/d_h)^{-0.346}$	Fan et al. [68]
for dispersed large bubble regime: $\epsilon_g = 1.81Fr_g^{0.222}Re_L^{0.432}M_o^{0.02}$	Song et al. [50]
for transition regime: $\epsilon_g = 0.654Fr_g^{0.358}Re_L^{0.051}M_o^{0.02}$	
for dispersed small bubble regime : $\epsilon_g = 2.61Fr_g^{0.21}Re_L^{-0.372}M_o^{0.02}$	
Middle and high gas holdup regions: $\epsilon_g = 0.814Fr_g^{0.3987}Re_L^{-0.0977}$	Gorowara et al. [69]
transition regime: $\epsilon_g = 0.132Fr_g^{0.285}Re_L^{-0.0895}$	
Homogeneous bubble flow regime: $\epsilon_g = 12A_r^{-0.23}B_o^{0.81}Fr_g^{0.51}(U_L/U_g)^{-0.19}(1 - \epsilon_s)^{1.47}(1 + 0.91x)^{1.59}$	Chen et al. [70]
Transition regime: $\epsilon_g = 19.2A_r^{-0.35}B_o^{0.74}Fr_g^{0.24}(U_L/U_g)^{-0.13}(1 - \epsilon_s)^{1.8}(1 + 0.91x)^{1.6}$	
Turbulent bubble flow regime: $\epsilon_g = 22.9A_r^{-0.37}B_o^{0.69}Fr_g^{0.14}(U_L/U_g)^{-0.11}(1 - \epsilon_s)^{1.87}(1 + 0.91x)^{1.63}$	
$\epsilon_g = 0.0139Re_g^{0.426}$	Safoniuk et al. [71]
$\epsilon_g = 0.11Fr_g^{0.35}Re_L^{0.2}M_o^{0.075}Ar_1^{0.11}$	Ramesh et al. [53]
$\epsilon_g = 0.4008Fr_g^{0.38547}Re_L^{-0.6712}$	Vinod et al. [72]
$\epsilon_g = 0.23U_g^{0.3}(gu_g)^{-0.1}$	Bakopoulos [73]
$\epsilon_g = \epsilon \left[ \frac{U_g - U_{gl}}{U_g - U_l} \right]$	Nacef et al. [74]
$\epsilon_g = 0.15U_L^{-0.047}U_g^{0.303}\epsilon_s^{-0.05}$	Son et al. [75]
$\epsilon_g = 0.0034Re_g^{0.7582}Re_L^{-0.14497}$	Jena et al. [66]
$\epsilon_g = 0.0023Re_g^{0.73}$	Jena et al. [29]
$\epsilon_g = 0.015U_g^{0.98}$	Abdel-Aziz et al. [76]
$\epsilon_g = 0.256Fr_g^{0.081}Re_L^{0.067}(P/D_c)^{0.79}(d_p/D_c)^{0.85}$	Kumar et al. [33]

Sulaymon et al.[38] Investigated the effect of bubble column operating conditions on liquid physical parameters, finding that the liquid circulation phenomena are visible for very viscous Newtonian and non-Newtonian liquids. Gas-holdup increases with increasing superficial gas velocity in three-phase fluidized beds for all particle sizes studied. When the superficial gas velocity exceeds 0.12 m/s, more complex hydrodynamic behavior develops, with the transition from bubbly to churn-turbulent flow regime. Furthermore, due to the coalescence process, large bubbles with a high bubble rise velocity were generated.[38]. Kumar et al. [33] studied the impact of several significant dynamic and geometric variables on individual phase holdups in a three-phase fluidized bed with a string of spheres promoter in the presence of a string of spheres promoter. Data on pressure drop was used to compute gas holdup. The gas holdup was observed to increase when gas velocity, pitch, and particle diameter increased. The gas holdup was unaffected by liquid velocity and rod diameter.

## 5. Heat Transfer in Three-Phase Fluidized Beds

The most crucial benefit of (gas-liquid-solid fluidized-bed systems) over a phase flow is the greatly enhanced heat transfer rates. The solid particles stir up the thermal boundary layer, increasing the heat transfer coefficient to eight times higher than single-phase forced convection. [77].

The heat transfer coefficient in a fluidized bed can be classified into five modes. Namely :(i) particle-particle, (ii) fluid-particle, (iii) bed to wall, (iv) heater to solid particle (v) heater to fluid. It is challenging to reach one general link for each heat transfer in a fluidized layer because each of the three modes is controlled by special interactive parameters.

The reaction temperature has been efficiently regulated by cooling or heating the column wall in a fluidized bed. Increased reaction conversion can be attained in three-phase fluidized beds due to higher mass and heat transfer rates due to aggressive solids mixing. The one with solid particles fluidized by co-current gas and liquid flow appears to be the basic mode of operation among the several types of three-phase contracting processes. Table 6 describes experimental conditions in previous heat transfer studies in three-phase fluidized beds. The heat transfer studies are classified into two groups in three-phase fluidized beds. One deals with heat transfer from wall to bed (Kato et al., [78], Muroyama et al., [79], Nore et al., [80], Zorana et al. [81]), and the other deals with heat transfer from immersed heat to bed (Baker et al. [82], Khan et al., [83], Magiliotou et al. [84], Luo et al., [85], Muroyama et al., [86], Grace et al., [87]). While most of these experiments contributed to the correlation of equations for the experimental results, some studied the processes mathematically and suggested a heat transfer mechanism. In addition, flat plate heaters (Khan et al., [83] and Luo et al., [85]) and cylindrical heat transfer studies (Baker et al. [82], Magiliotou et al., [84], and Muroyama et al., [86]) were used [88].

Many studies have looked into the effects of gas velocity on heat transfer rate in two and three-phase systems (Baker et al. [82]; Chiu et al., [77]; Kang et al. [89]). These results indicated that the rate of increase in heat transfer coefficients with gas velocity was rapid at low gas velocity, and then decreased as gas velocity increased. Several studies have looked into the effects of liquid velocities on heat transfer coefficients in two and three-phase fluidized beds, including (Kato et al., [78]; Kim et al. [90]; Kumar et al., [91]).

The results of previous studies show that the heat transfer coefficient increases initially. As a function of increasing liquid velocity, it reaches the maximum value and then drops. Lin et al. [4] used a particle image analyzer (PIA) and a heat transfer probe to quantitatively study the macroscopic hydrodynamics and heat transfer of a two-dimensional (2D) three-phase fluidized bed. Different solid holdups are added to the flow to investigate the influence of solid holdups on heat transfer. It has been discovered that solid particles can increase the collision frequency between solid particles and the heating object, resulting in increased heat transfer. Kang et al. [75] observed that the average boundary layer thickness around the heater might drop in a three-phase circulating fluidized bed heat transfer system as gas velocity increases. Higher  $U_g$  may induce more bubble holdup and turbulence, allowing the fluid element in the riser to attack the boundary layer around the heater surface. At varied operating conditions, Abdul-Wahab et al. [88] measured the heat transfer rate and overall temperature differential across the heater. The temperature profiles were calculated axially and radially for different positions in the bed. The differential equation describing heat transfer in a gas-liquid-solid fluidized system with boundary conditions has been solved using theoretical analysis. Table 6: Previous heat transfer condition experimental three-phase investigation fluidized beds.

Practical thermal conductivity values were calculated using the solved equation's temperature profiles. Lim et al. [100] obtained that the heat transfer coefficient ( $h$ ) between the immersed vertical heater and the riser suitable for the three-phase circulating fluidized bed increased as the gas and liquid velocities increased but did not affect much when the liquid velocity increased in the upper range. The heat transfer coefficient increased gradually as the size of fluidized solid particles increased without reaching a local minimum, indicating that bed contraction in three-phase circulating fluidized beds was not caused by increasing liquid velocity. The heat transfer systems may more easily achieve a stable condition with larger particle size. Arsenijević et al. [99] investigated and correlated the heat transfer coefficient between the hot air and the cooling water. The works were carried out with various fluid flow rates and inlet air temperatures while keeping the air flow rate constant. A new correlation for heat transfer in a three-phase fluidized system was developed based on the experimental results. In most heat transfer studies, the  $h$  has been determined by measuring the temperature differences between the heating surface and the bulk flow region of the fluidized bed.

### 5.1 Heat Transfer Coefficient in Three-Phase Fluidized Beds (H)

It is essential to understand the heat transfer coefficient while designing heat transfer in a fluidized-bed system. The fact that it depends on a wide variety of system characteristics and operations makes calculating the acceptable value for the transfer heat coefficient difficult. The parameters are gas and liquid velocity, liquid viscosity, particle size and density, slurry concentration, bed porosity, column diameter, heat transfer section/axial probes, and radial position. Chiu and Ziegler suggested a fluidized bed's heat resistance model. This means that there are two heat transfer resistances near the heating surface and the other within the bed. The heat transfer coefficient ( $h$ ) was determined using the following equation:

$$h = \frac{q}{A(T_s - T_b)} \quad (7)$$

Where  $T_b$  and  $T_s$  are the bed's temperatures and the heater surface's temperature, respectively. The DC power supply provided the heat supply ( $q$ ).

Several empirical correlations to heat transfer coefficients have been proposed based on the heat transfer coefficient measurement between the immersed heating surfaces and the bed.

Table 7 summarizes previous heat transfer studies' proposed correlations for predicting  $h$  in three-phase fluidized beds.

Cao et al. [105] simulated a gas-liquid-solid circulating fluidized bed using two-dimensional Eulerian-Eulerian-Lagrangian (E/E/L) approaches. They combined the E/E/L model with the Two-Fluid Model (TFM) and the Distinct Element Method (DEM). The generalized gas-liquid two fluids k-model forms the modified gas-liquid TFM. As shown in Figures 9-11, they investigated the radial distribution of local phase hold-ups and local liquid velocity.



**Table 7:** The literature's main correlations for heat transfer coefficients

Correlation	Ref.
$h = 1977 U_g^{0.059} U_L^{0.07} d_p^{0.106}$	Baker et al. [82]
$h = 0.075 k_L^{0.5} \rho_L^{0.75} c_{pL}^{0.5} \mu_L^{-0.27} g^{0.25} (U_g - U_L)^{0.25}$	Deckwer et.al. [101]
$h = 1304 U_g^{0.22} U_L^{0.01} \mu_L^{-0.31}$	Kang et al. [89]
$h = C(k_L \rho_L c_{pL} \{[(U_L+U_g) (\rho_g \varepsilon_{Lg} + \rho_L \varepsilon_L + \rho_s \varepsilon_s) - \rho_L U_L] g / (\varepsilon_L \mu_L)\}^{0.5})^{0.5}$	Kim et al. [90]
$Nu = 0.042 Re_L^{0.72} Pr_L^{0.86} Fr_C^{0.067}$	Zaidi et al. [102]
$h = [h' \varepsilon_g^{0.45} + \left( \frac{0.396}{U_g^{0.45}} - \frac{0.6768}{U_{pt,0}} \right)]$	Luo et al. [85]
$h = 2776 U_g^{0.0779} U_L^{0.0317} G_s^{0.0654}$	Cho et al. [97]
$h = 0.042 (k_L \rho_L c_{pL} \{[(U_L+U_g) (\rho_g \varepsilon_{Lg} + \rho_L \varepsilon_L + \rho_s \varepsilon_s) - \rho_L U_L] g / (\varepsilon_L \mu_L)\}^{0.5})^{0.5}$	Patnaik. [98]
$h = 2552 U_g^{0.21} U_L^{0.03} G_s^{0.0654} d_p^{0.05} \sigma_L^{-0.08}$	Lim et al. [100]
$Nu_p = 0.042 Re_p Pr_L^{0.333} j_{HP}$	Arsenijević et al. [99]
$h = 0.19 U_g^{0.76} \mu_L^{0.155}$	Abdel-Aziz et al. [76]

## 6. Computational Fluid Dynamics (CFD)

As computing power increases, numerical simulation has become a more powerful technique for predicting fluid dynamics and heat transfer mechanisms in multi-phase flow. To simulate the liquid/gas fluidized bed, a numerical hydrodynamic and heat transport model was constructed. CFD is based on the fundamental governing equations of fluid dynamics in some form or another (continuity, momentum, and energy equations). These are physics equations. They are mathematical expressions of three essential physical principles that underpin all fluid dynamics: mass conservation, Newton's second law, and energy conservation. The availability of high-performance computing hardware and the invention of user-friendly interfaces have facilitated the development of CFD software for both commercial and scientific purposes. Some general-purpose CFD packages used are PHONICS, CFX, FLUENT, FLOW3D, and STAR-CD. These packages use finite volume techniques to analyze fluid flow, heat transfer, and mass transfer problems [12]. The two primary approaches are the Euler-Euler formulation, which will depend on the interfacial multifluid model, and the Euler-Lagrangian formulation, which is based on solving Newton's equation of motion for the dispersed phase.

### 6.1 Studies on Three-Phase Fluidized Beds Using Computational Fluid Dynamic

There have been many computational studies throughout the years, but more work in CFD is required for the extensive range of experimental data available. The validity of CFD predictions may be validated by comparing them to experimental data and results. Due to the time-consuming nature of practical work, CFD aids in predicting fluid flow, fluidized bed behavior, and various hydrodynamic properties. CFD helps in modeling a real-world process prototype, and it is possible to use those parameters to get the desired results using CFD simulations. CFD could be used to understand the complicated hydrodynamics of fluidization [103]. Table 8 contains an extensive overview of the literature on modeling these reactors. These CFD investigations use a steady-state, two-dimensional, Eulerian multifluid technique. However, three-phase flows in fluidized bed reactors are extremely unstable, as they are thought up of many flow processes that occur at various time and length scales.

Feng et al.[36] Developed a three-dimensional computational fluid dynamic (CFD) model to predict the structure of the three-phase flow of gas, liquid, and TiO<sub>2</sub> nanoparticles in the bubble column. The time-averaged and time-dependent predictions were compared to experimental data for model validation. Immediate local gas holdup, gas velocity, and liquid velocity were also accurately predicted. All of this will be shown in detail in figures 3–8.

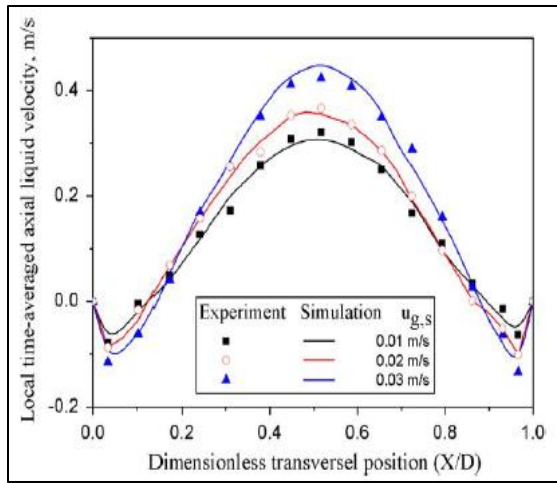


**Figure 3:** Effects of superficial gas velocity ( $U_{g,s}$ ) on local time-averaged axial liquid velocity,  $\alpha_s = 3.3\%$ ,  $Z/D=2.0$ [36].

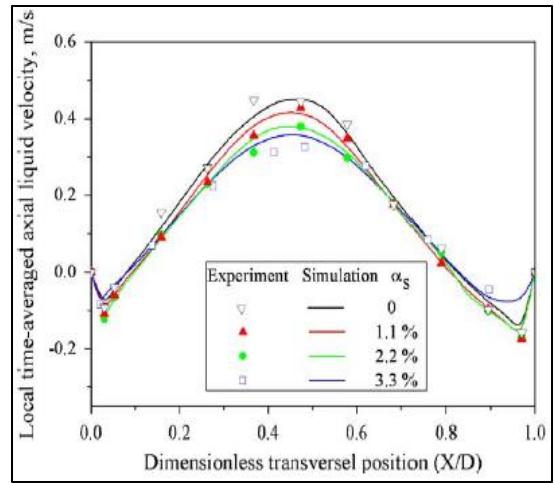


**Figure 4:** Effects of Nanoparticles ( $\alpha_s$ ) on the local time-averaged axial liquid velocity,  $U_{g,s} = 0.02\text{ m/s}$ ,  $Z/D=2.0$ [36].

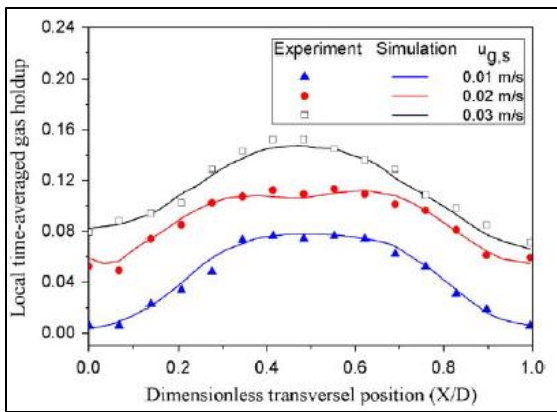


**Figure 5:** Effects of superficial gas velocity ( $U_{g,s}$ ) on the local time-averaged gas holdup,  $\alpha_s = 3.3\%$ ,  $Z/D=2.0$ [36].

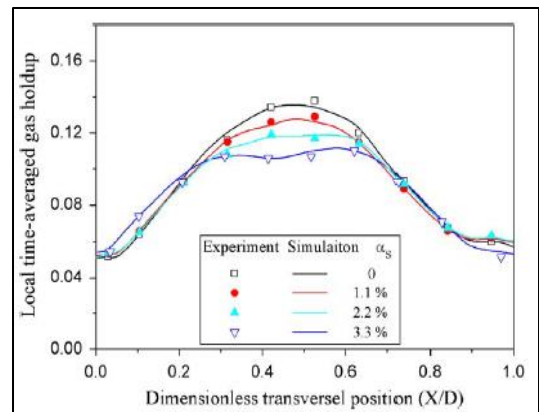


**Figure 6:** Effects of Nanoparticles loading ( $\alpha_s$ ) on the local time-averaged gas holdup,  $U_{g,s} = 0.02\text{ m/s}$ ,  $Z/D=2.0$ [36].

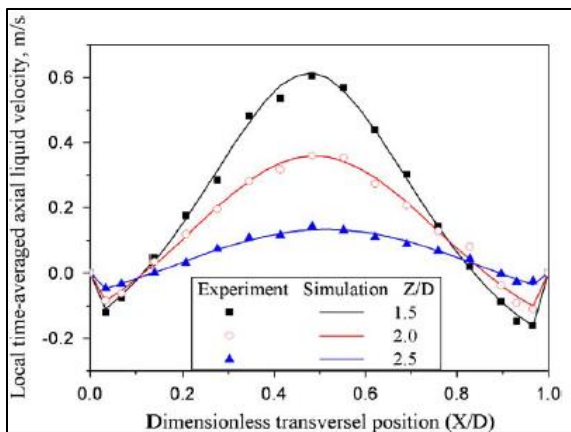


**Figure 7:** Effects of dimensionless axial position ( $Z/D$ ) on the local time-averaged axial liquid velocity,  $U_{g,s} = 0.02\text{ m/s}$ ,  $\alpha_s = 3.3\%$ [36].

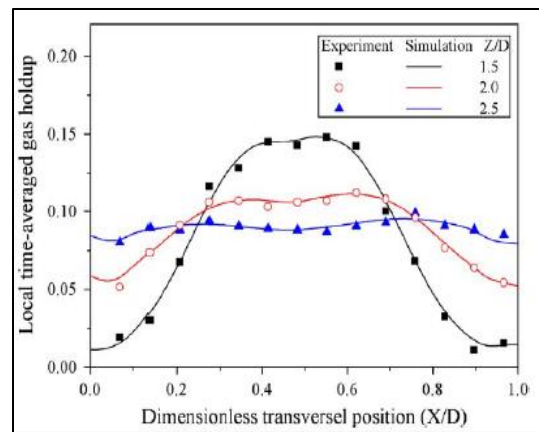


**Figure 8:** Effects of dimensionless axial position ( $Z/D$ ) on the local time-averaged gas holdup,  $U_{g,s} = 0.02\text{ m/s}$ ,  $\alpha_s = 3.3\%$ [36].

**Table 8:** Summarizes research on three-phase reactor CFD modeling.

<i>Parameter investigated</i>	<i>Fluidizing medium</i>		<i>solid</i>	<i>Multi-phase approach</i>	<i>Remarks of study</i>	<i>Ref.</i>
	<i>Gas</i>	<i>Liquid</i>				
The local time-averaged liquid velocity and gas holdup profiles were compared with the radial position.	Air	Water	TiO2 nanoparticles	3-D, Multi-fluid, Eulerian-Eulerian technique is used For a three-phase bubble column.	Developed to predict the flow pattern of three-phase gas-liquid-nanoparticles flow bubble column reactors.	Feng et al.[36]
The radial distribution of local phase hold-ups and the local liquid velocity was examined.	Air	Carboxy-methyl cellulose sodium	styrene resin	2-D, Eulerian-Lagrangian model for gas-liquid-solid circulating fluidized bed	The significance of accurately modeling the direct interactions between dispersed gas and solid phases in a three-phase system was proved.	Cao et al.[104]
The overall performance of a fluidized gas-liquid-solid bed and averaged solid velocity profile's predicted flow pattern.	Air	Water	Glass beads, polyvinyl chloride	3-D, Multiphase Flow, Eulerian- the Eulerian approach is applied to a three-phase fluidized bed reactor.	The averaged solid velocity profile's predicted flow pattern indicates a higher upward velocity in the column's central region and a lower low rate in the column's wall region.	Panneerselvam et al. [105]
Identify the turbulence models' effect. Furthermore, the impact of numerical schemes, such as two-dimensional versus three-dimensional models.	Air	Water	Glass beads, polyvinyl chloride	3-D, unsteady multiple-Euler framework of gas-liquid-solid fluidized.	A laminar model formulation accounting for the two fluids' solid phase and molecular viscosities produced the best flow characteristics prediction.	Hamidipour et al. [106]
The bed expansion and gas holdup of a fluidized bed with and without a distributor plate were compared.	Air	Water	Plastic beads	2-D,3-D, multifluid Eulerian approach for three-phase fluidized bed column	A fluidized bed with a distributor has higher bed expansion and gas holdup values than a fluidized bed without a distributor plate.	Mishra [12]
Examine the three-phase phase bubble columns' hydrodynamics.	Air	Water	Glass powder	Three-fluid The KTGP utilizes an Eulerian-Eulerian approach.	The hydrodynamic parameters were highly influenced by dp and Vs. The axial solid concentration gradient was higher when the values of Vs, dp, and ρp were larger.	Li et al. [107]
The behavior of gas and liquid hold-up has been extensively investigated.	Air	Water	Glass beads	2-D, Eulerian-Eulerian technique with the CFD software package STAR-CCM+ CFD is applied. For the three-phase fluidization system,	In the fluidized region of the column, the volume fraction of water is lower than in the rest. At constant water velocity, gas holdup increases as air velocity increases. At constant air velocity, gas holdup decreases as inlet water velocity increases.	Saha et al.[108]
hydrodynamics and flow structures in a batch liquid mode inverse three-phase fluidized bed	Air	Water	Polypropylene, polyethylene	2-D, Multi-fluid, Eulerian-Eulerian (E-E) approach is used For an inverse three-phase fluidized bed column.	Based on the axial profile of the solid phase, the flow development in the inverse three-phase fluidization system can be classified into three stages: initial fluidization, developing stage, and fully developed stage. A more significant solids volume fraction occurs at all three stages when particles flow upward, and a smaller volume fraction occurs when particles flow downward.	Liu et al.[109]

Cao et al. [104] simulated a gas-liquid-solid circulating fluidized bed using two-dimensional Eulerian–Eulerian-Lagrangian (E/E/L) approaches. They combined the E/E/L model with the Two-Fluid Model (TFM) and the Distinct Element Method (DEM). The generalized gas-liquid two fluids k-model forms the modified gas-liquid TFM. As shown in Figures 9-11, they investigated the radial distribution of local phase hold-ups and local liquid velocity.

Mishra[12] utilized a multi-phase model by using ANSYS Fluent 13.0, a commercial CFD package, to simulate the system. The inter-phase drag force was calculated using the Gidaspow and Schiller-Neumann drag models. The turbulent quantities were described using a two-equation standard k-model. No literature on three-phase fluidized bed systems with a distributor plate is simulated using CFD. The current research investigated a fluidized bed with a distributor with a diameter of 0.002 m orifice. Compared to a fluidized bed without a distributor plate, the simulation results reveal that a fluidized bed with a distributor has more significant bed expansion and gas holdup values. Figures 12 to 15 show some of the results obtained from the hydrodynamics of the three-phase phase bubble columns. Li et al. [107] developed CFD simulation employing the three-fluid Eulerian-Eulerian technique with the KTGP. The liquid phase was modeled using the distributed RNG model. Even with variable surface gas velocities, a mean bubble size was used. The interphase force, which includes the drag force, was investigated for its sensitivity. The best drag model for liquid and solid phases was the Schiller-Naumann drag [109], and the drag force between the gas and solid phases was not properly considered. The effect of superficial gas velocity, particle density, solids loading, and particle size on the hydrodynamics of a three-phase bubble column is investigated based on CFD results. Khongprom et al. [110] used CFD simulation to study the effect of particle characteristics on the flow behavior in the gas-liquid-solid bubble column. The kinetic theory of granular flow and a multifluid model was used. Particle sizes of 3 mm, 4

mm, and 5 mm were investigated, as well as particle densities of 2,250 kg/m<sup>3</sup>, 2,450 kg/m<sup>3</sup>, and 2,750 kg/m<sup>3</sup>. The findings revealed that particle size significantly impacted hydrodynamic and radial uniformity. The flow behavior of micro particles is very unstable, with less regularity in the radial direction. It was possible to achieve a robust turbulent regime. For large particles, the flow behavior becomes more uniform. Many papers have been published on the theoretical and experimental studies of three-phase FBRs. Still, little attention has been given to the CFD approach to three-phase fluidization systems. The Zhang-Vanderheyden model was the best drag model for liquid and gas phases [111].

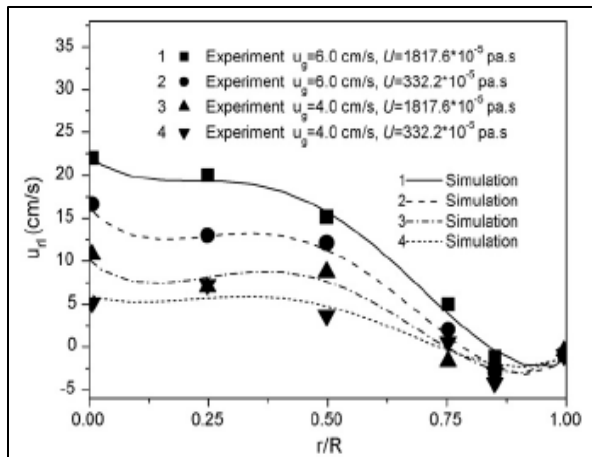


**Figure 9:** A comparison of CFD predicted and experimental local liquid velocity radial profiles for various superficial gas velocities, 0.6m above the gas distributor, 4 kg/(m<sup>2</sup>s) solid circulation rate, superficial liquid velocity 4.0 cm/s, air–SCMC–styrene resin system[104]

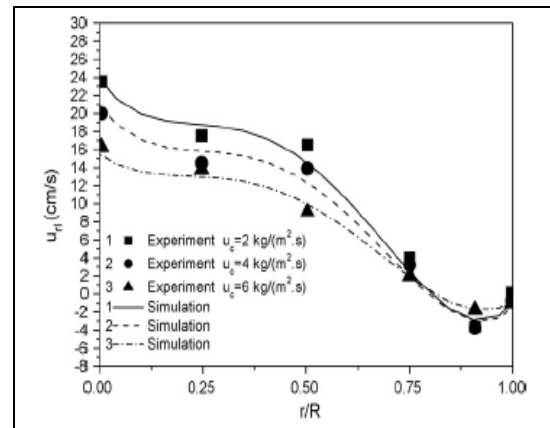


**Figure 10:** Experimental and predicted local liquid velocity radial profiles for various solid circulation rates, 0.6m above gas distributor, superficial gas velocity 4 cm/s, superficial liquid velocity 5.0 cm/s, air–0.05 % SCMC–styrene resin system[104]

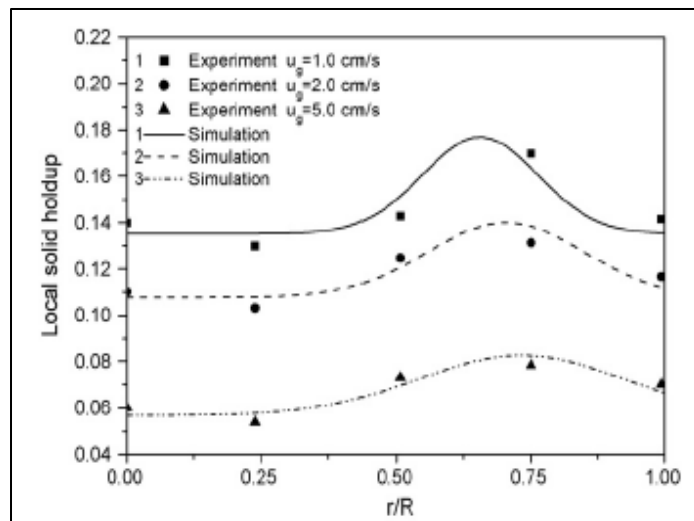


**Figure 11:** A comparison of CFD predicted and experimental local solid hold-up radial profiles for various superficial gas velocities, 0.6m above gas distributor, 6 kg/ (m<sup>2</sup> s) solid circulation rate, 2.0 cm/s superficial liquid velocity, air–0.05 % SCMC–styrene resin system[104]

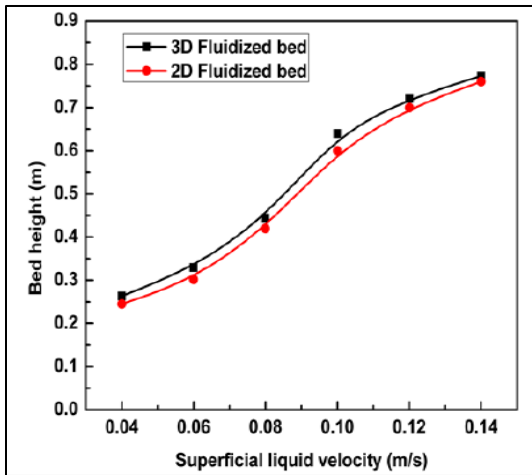


**Figure 12:** Illustrates the comparison in bed height between a 2D and a 3D fluidized bed without a distributor[12]

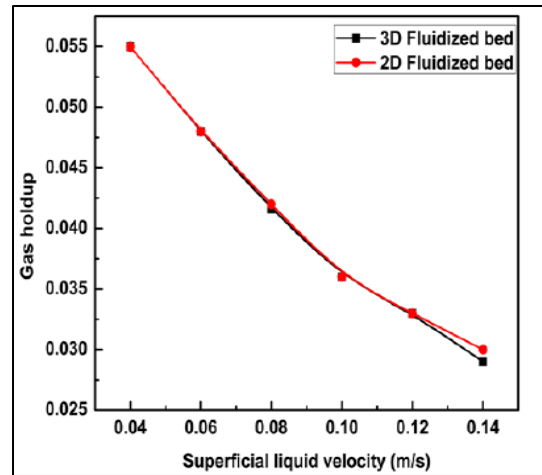


**Figure 13:** Without a distributor, compare the gas holdup of 2D and 3D fluidized beds [12]

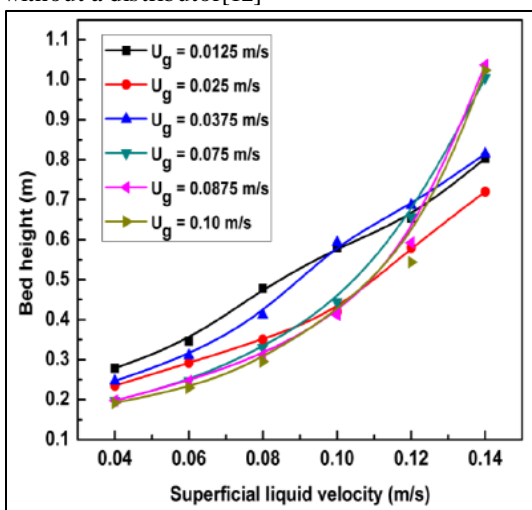


**Figure 14:** CFD simulation of bed expansion behavior of 2.18 mm glass beads in a 3D fluidized bed with a static bed height of 0.213 m and constant gas velocity [12]

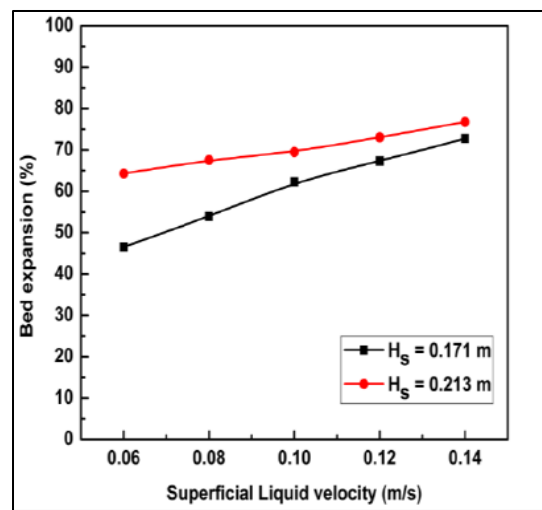


**Figure 15:** Bed height derived from a CFD simulation of a 2D fluidized bed with a distributor at various static bed heights [12]

## 7. Conclusions

There has been a brief discussion of current hydrodynamic behavior and heat transfer studies in a fluidized bed. The different techniques for analyzing hydrodynamic parameters, heat transfer in fluidized beds, and the performance characteristics that influence hydrodynamic and heat transfer in the bed and fluidized bed performance have been discussed. The survey arrives at the following conclusions:

- Developing optimal design and operating techniques for three-phase fluidized-bed operations is critically needed. To that aim, new design configurations of the three-phase fluidized bed and associated fundamental analysis are required. When using a three-phase fluidized bed as a chemical or biochemical reactor, the main aim of novel design configurations is to obtain maximal mass and heat transfer effects with minimal power input while maintaining optimal fluid mixing for specified reaction kinetics.
- This uniform correlation of hydrodynamic and heat transfer parameters applies to a wide range of operational modes. This unifying correlation applies to incipient fluidization in a three-phase fluidized bed reactor with Newtonian and non-Newtonian fluids.
- Controlling parameters such as the superficial liquid velocity, superficial gas velocity, particle size, bed geometry, bed peak temperature, suspension density, and heat transfer coefficient affect hydrodynamic performance and heat transfer phenomena. Because their impact on bed performance changes from bed to bed and phase to phase, it cannot be established that their effects on heat transfer and hydrodynamic performance output are constant. As a result, different bed geometry and designs may have varying heat transfers and hydrodynamic behavior.
- According to the literature, only a few studies have concentrated on developing CFD models for the three-phase fluidization process based on a three-fluid Eulerian-Eulerian technique. Most CFD models are for upward TPFBs. The

hydrodynamics and flow patterns in a three-phase fluidized bed were studied using a CFD model. A correlation was proposed to estimate the volume fraction, average liquid holdup, average gas holdup, particle velocity, and fluid velocity. There are still other areas that can be researched further using CFD to better understand the hydrodynamics of TPFB.

### Author Contribution

Methodology, Omar S. Mahdy, Amer A. Abdulrahman, and Jamal M. Ali.; software, Omar S. Mahdy.; validation, Amer A. Abdulrahman, and Jamal M. Ali.; formal analysis, Jamal M. Ali.; writing—original draft preparation, Omar S. Mahdy.; writing—review and editing, Omar S. Mahdy, Amer A. Abdulrahman, and Jamal M. Ali.; supervision, Amer A. Abdulrahman, and Jamal M. Ali.; project administration, Amer A. Abdulrahman.; All authors have read and agreed to the published version of the manuscript.

### Funding

This research received no external funding.

### Data Availability Statement

In this section, please provide details regarding where data supporting reported results can be found, including links to publicly archived datasets analyzed or generated during the study. You might exclude this statement if the study did not report any data.

### Conflicts of Interest

The authors declare no conflict of interest.

### Nomenclature

Symbol	Description	SI unit
CFD	Computational fluid dynamics	-
$\Delta P$	Pressure drop throughout the bed	Kpa
$U_{mf}$	Minimum fluidization velocity	m/s
$\beta_{er}$	Bed expansion ratio	-
$U_{cd}$	transition liquid velocity from the coalesced to dispersed bubble regime	m/s
$U_b$	Bubble rise velocity	m/s
$U$	Phase velocity	m/s
$R$	radius of the bed m	m
$r_p$	radial position	m
$r$	Bed fluctuation ratio	-
CMCS sol.	carboxymethyl cellulose sodium solution	-
CMC sol,	carboxymethyl cellulose solution	-
$U_{gmf}$	Minimum gas fluidization velocity	m/s
EPS	Expanded polystyrene	-
BOD	Biochemical oxygen demand	-
COD	Chemical oxygen demand	-
$d_p$	Particle diameter	m
IGLSCFB	Inverse gas-liquid-solid circulating fluidized bed	-
ILSCFB	Inverse liquid-solid circulating fluidized bed	-
TPFB-S	Spiral three-phase fluidized bed reactor	-
SEM	Scanning electron microscope	-
FTIR	Fourier transform infrared spectroscopy	-
RC	Ricinus communis particle	-
TPFB	three-phase fluidized bed reactor TPFB	-
$D_c$	Column diameter	m
$U_L$	Velocity of the liquid	m/s
$U_g$	Velocity of the gas	m/s
$H_c$	Height of the column	m
$g$	Gravitational acceleration	m/s <sup>2</sup>
$U_{Lmf}$	Minimum liquid fluidization velocity	m/s
$U_{Lmf}^{L.s}$	Minimum liquid fluidization velocity for L-S fluidized bed	m/s
$M_s$	Solid mass of the column	kg
$A_c$	Cross-sectional area of the column	m <sup>2</sup>
$H_e$	Expanded bed height	m

$D_h$	Inner diameter of the miniaturized fluidized bed	m
$H_s$	static bed height	m
$O_l$	Liquid surface tension	N/m
RSM	Response surface methodology	-
$x$	ratio of solid holdup in wake region to that in the liquid-solid fluidized bed region	-
LDA	Laser Doppler anemometer	-
PIA	Particle image analyzer	-
2D	Two-dimensional	-
3D	Three-dimensional	-
$h$	Total average heat transfer coefficient	W/m <sup>2</sup> .K
$q$	Amount of heat supply	W
$T_b$	Temperatures of the bed	K
$T_s$	Temperature of the heater surface	K
$C_p$	Specific heat at constant pressure	J/kg. K
$K$	Thermal conductivity of liquid phase	J/m.s. K
$c$	proportionality constant	-
$G_s$	Dimensionless solids circulations rate	-
$h'$	heat-transfer coefficient of a liquid-solid fluidized bed with the same solid's holdup	W/m <sup>2</sup> .K
$j_{HP}$	heat transfer factor	-
$U_{pt,0}$	particle terminal velocity in the fluidizing liquid at the ambient pressure	m/s
$U_{g,s}$	superficial gas velocity,	m/s
$Z$	Z-direction (axial) position	m
$Z/D$	dimensionless axial position	-
<b>Greek Letters</b>		
$\beta_{er}$	Bed expansion ratio	-
$\epsilon_g$	Gas holdup	-
$\epsilon_L$	liquid holdup	-
$\epsilon_s$	Solid holdup	-
$\epsilon$	Porosity	-
$\rho$	Density	Kg/m <sup>3</sup>
$\epsilon_{mf}$	void fraction at the point of minimum fluidization	-
$\phi_s$	sphericity of the solid particle	-
$\mu$	viscosity	N.s/ m <sup>2</sup>
$\sigma$	Surface tension	N/m
$\alpha$	volume fraction in the liquid-nanoparticles suspension, dimensionless	-

### Dimensionless Groups

$$Ar \quad \text{Archimedes number} = \left[ \frac{d_p^3 \rho_l (\rho_s - \rho_l) g}{\mu_l^2} \right]$$

$$Pr \quad Prandtl \ number = \left[ \frac{\mu_l C_p l}{k_l} \right]$$

$$Re_p \quad Particle \ Reynolds \ number = \left[ \frac{\rho_l U d_p}{\mu_l} \right]$$

$$F_r \quad Froude \ number = \left[ \frac{u_{mf}^2}{d_p g} \right]$$

$$Mo \quad Morton \ number = \left[ \frac{\mu_l 4g}{\rho_l \sigma} \right]$$

$$Nu \quad Nusslet \ number = \left[ \frac{hd_p}{k} \right]$$

### Subscript

g	gas
L	Liquid
mf	at minimum fluidization conditions for gas-solid/liquid-solid system
Lmf	At minimum fluidization conditions for the liquid
gmf	At minimum fluidization conditions for the gas
m	Modified
s	solid
p	particle
S	surface
P	pitch

### References

- [1] C. Chen and L. Fan, Discrete simulation of gas-liquid bubble columns and gas-liquid-solid fluidized beds, *AIChE Journal* 50, 2 (2004) 288–301. <http://doi.org/10.1002/aic.10027>
- [2] H.M. Jena, Hydrodynamics of gas-liquid-solid fluidized and semi-fluidized beds, Ph.D. Thesis Submitt. to Natl. Inst. Technol. Rourkela, (2009).
- [3] J. M. Begovich and J. S. Watson., Hydrodynamic characteristics of three-phase fluidized beds., Cambridge Univ. Press. Cambridge, 3 (1978) 190-195.
- [4] T. J. Lin and C. Hung-Tzu, Effects of macroscopic hydrodynamics on heat transfer in a three-phase fluidized bed, *Catal. Today*, 79–80 (2003) 159–167. [http://doi:10.1016/S0920-5861\(03\)00021-X](http://doi:10.1016/S0920-5861(03)00021-X).
- [5] Y. Shao, J. Gu, W. Zhong, and A. Yu, Determination of minimum fluidization velocity in a fluidized bed at elevated pressures and temperatures using CFD simulations, 350 (2019) 81–90. <http://doi:10.1016/j.powtec.2019.03.039>.
- [6] M. A. Thombare, P. V Chavan, S. B. Bankar, and D. V Kalaga, Solid-liquid circulating fluidized bed : a way forward, *Rev Chem Eng*, 2017; (2017). <http://doi:10.1515/revce-2017-0017>.
- [7] K.Muroyama and L. Fan, Fundamentals of gas- liquid -solid fluidization, *AIChE Journal* , 31, 1 (1985).
- [8] A. Pare, Hydrodynamics of three phase fluidized bed using low density particles, M.C.S. Thesis Submitt. To Department of Chemical Engineering National Institute of Technology Rourkela, (2013).
- [9] R. Cocco, S. B. Reddy, and K. T. Knowlton, Introduction to fluidization., *AIChE Journal*, (2014) 21–29.
- [10] E. Ramaswamy, C. Sirinivasakaan, and N. Balasubramaniam. Bed expansion characteristics of liquid-solid fluidized bed with internals, *Modern Applied Science* 2.2 (2008): 84-92. <http://doi:10.5539/mas.v2n2p84>.
- [11] Y. H. Kim, A. Tsutsumi, and K. Yoshida, Effect of particle size on gas holdup in three-phase reactors, *Sadhana* 10.1 (1987): 261-268. <http://doi.org/10.1007/BF02816208>.
- [12] S. Mishra, Hydrodynamic Studies of Three-Phase Fluidized Bed by Experiment and CFD Analysis, Ph.D.Thesis July, (2014).
- [13] D. Sinha, R.Baliyan, A. Rana ,and R. Israni, Hydrodynamics of three phase fluidized bed using low density particles, *IJARIE-ISSN(O)-2395-4396*, 2 (2016) 236–244.
- [14] S. Hembram, Behaviour of Three Phase Fluidized Bed with Regular Particles, PhD thesis, 108 (2013).

- [15] R. K. Padhi., Prediction of bed pressure drop , fluctuation and expansion ratios for three-phase fluidization of ternary mixtures of dolomite in a conical conduit Cogent Eng., 23 (2016) <http://doi:10.1080/23311916.2016.1181821>.
- [16] G. Sun, and J. R. Grace, Effect of Particle Size Distribution in Different Fluidization Regimes, AIChE journal 38 (1992) 716-722. <http://doi.org/10.1002/aic.690380508>.
- [17] R. Sukarsono, S. Riyadi, and D. H. S. Rinanti, The selection of geometry and flow rate on the fluidized bed reactor for coating particle, IOP Conf. Series: Journal of Physics: Conf. Series 1198 (2019). <http://doi:10.1088/1742-6596/1198/2/022079>.
- [18] K. Sivaguru, K. M. M. S. Begum, and N. Anantharaman, Hydrodynamic studies on three-phase fluidized bed using CFD analysis, 155 (2009) 207–214. <http://doi:10.1016/j.ccej.2009.07.037>.
- [19] N. Love and A. Choudhuri, Effect of bed height, bed diameter and particle shape on minimum fluidization in a gas-solid fluidized bed, Conference Paper, (2012). <http://doi:10.2514/6.2012-644>.
- [20] P. Sahoo and A. Sahoo, Fluidization and spouting of fine particles : A comparison, Advances in Materials Science and Engineering, (2013), Article ID 369380, 7 pages, 2013. <http://doi.org/10.1155/2013/369380>.
- [21] P. Lettieri and D. Macrì, Effect of process conditions on fluidization, KONA Powder and Particle Journal, review paper, (2015) 1-24. <http://doi:10.14356/kona.2016017>.
- [22] H. Bodhanwalla, M. Ramachandran, and S. S. Nmims, Parameters affecting the fluidized bed performance : A review REST Journal on Emerging trends in Modelling and Manufacturing., 3 (2017).
- [23] M. Down more and S. D. Jambgwa, Effect of bed particle size and temperature variation on the minimum fluidization velocity : A comparison with minimum fluidization velocity correlations for bubbling fluidized bed designs, 0 (2019) 1–12. <http://doi:10.1177/0954408918821769>.
- [24] F. Karachi, L. Belfares, I. Iliuta, and B. P. A. Grandjean, Three-phase fluidization macroscopic hydrodynamics revisited, Ind. Eng. Chem. Res., 40 (2001) 993–1008. <http://doi:10.1021/ie0006864>.
- [25] D. Lee, A. Macchi, N. Epstein, and J. R. Grace, Transition Velocities and Phase Holdups at Minimum Fluidization in Gas-Liquid-Solid Systems, The Canadian Journal of Chemical Engineering 79 (2001): 579-58. <http://doi.org/10.1002/cjce.5450790416>.
- [26] L. A. Briens and N. Ellis, Hydrodynamics of three-phase fluidized bed systems examined by statistical, fractal, chaos and wavelet analysis methods, Chem. Eng. Sci., 60 (2005) 6094–6106. <http://doi:10.1016/j.ces.2005.04.005>.
- [27] P. Dargar and A. Macchi, Effect of surface-active agents on the phase holdups of three-phase fluidized beds, 45 (2006) 764–772. <http://doi:10.1016/j.ccep.2006.03.004>.
- [28] C. Cao, M. Liu, and Q. Guo, Experimental investigation into the radial distribution of local phase holdups in a gas - liquid - solid fluidized bed, Industrial & engineering chemistry research 46.11 (2007) 3841-3848. <http://doi.org/10.1021/ie060798g>.
- [29] H. M. Jena, B. K. Sahoo, G. K. Roy, and B. C. Meikap, Characterization of hydrodynamic properties of a gas-liquid-solid three-phase fluidized bed with regular shape spherical glass bead particles, 145 (2008) 50–56. <http://doi.10.1016/j.ccej.2008.03.002>.
- [30] D. Zhou, S. Dong, H. Wang, and H. T. Bi, Minimum fluidization velocity of a three-phase conical fluidized bed in comparison to a cylindrical fluidized bed, Ind. Eng. Chem. Res., 48 (2009) 27–36. <http://doi:10.1021/ie8001974>.
- [31] A. Sivalingam and T. Kannadasan, Effect of fluid flow rates on hydrodynamic characteristics of co-current three-phase fluidized beds with spherical glass bead particles, Int. J. ChemTech Res., 1 (2009) 851–855.
- [32] Y. Li, M. Liu, and L. Yanjun, Minimum Fluidization Velocity in Gas-Liquid-Solid Minifluidized Beds, AIChE J., 62, 4 (2016) 1940–1957. <http://doi.org/10.1002/aic.15196>.
- [33] [33] P. Rohini Kumar, K. V Ramesh, and P. Venkateswarlu, Phase Holdups in A Three-Phase Fluidized Bed in the Presence of Coaxially Placed String of Spheres Internal, IOP Conf. Ser. Mater. Sci. Eng., 225 (2017). <http://doi:10.1088/1757-899x/225/1/012210>.
- [34] A. Sivalingam and T. Kannadasan, Effect of fluid flow rates on hydrodynamic characteristics of co-current three phase fluidized beds with spherical glass bead particles, Int. J. ChemTech Res., 1 (2009) 851–855.
- [35] A. Knesebeck and R. Guardani, Particle distribution in a three-phase fluidized bed under low-to-intermediate Reynolds conditions, 140 (2004) 30–39. <http://doi:10.1016/j.powtec.2003.12.013>.
- [36] W. Feng, J. Wen, J. Fan, Q. Yuan, X. Jia, and Y. Sun, Local hydrodynamics of gas – liquid-nanoparticles three-phase fluidization, 60 (2005) 6887–6898. <http://doi:10.1016/j.ces.2005.06.006>.

- [37] V. G. Aditya, P. Panda, S. C. Rana, and H. M. Jena, Experimental Study of the Behaviour of a Three-phase Fluidized Bed with Cylindrical Particles, (2006).
- [38] A. H. Sulaymon, T. J. Mohammed, and A. H. Jawad, Hydrodynamic Characteristics of Three-Phase Non-Newtonian Liquid-Gas-Solid Fluidized Beds, *Emirates J. Eng. Res.*, 15, 1 (2010) 41–49.
- [39] S. Venkatachalam, K. Kandasamy, and S. Kandasamy, Correlation for prediction of minimum fluidization velocity and riser liquid holdup in three-phase external loop airlift fluidized bed reactor, *Int. J. Chem. React. Eng.*, 8 (2010). <http://doi:10.2202/1542-6580.2337>.
- [40] T. J. Mohammed, A. H. Sulaymon, and A. A. Abdul-Rahmun, “Hydrodynamic Characteristic of Three-Phase (Liquid-Liquid-Solid) Fluidized Beds, *J. Chem. Eng. Process Technol.*, 5, 2 (2014). <http://doi:10.4172/2157-7048.1000188>.
- [41] T. Nan, Hydrodynamics of Liquid-Solid and Three-Phase Inverse Circulating Fluidized Beds, Electron. Ph. D Thesis Diss. Repos., Western Univ., (2019).
- [42] C. Calvachi, G. Lucía, and I. Ortiz, Recirculating aquaculture system with three phase fluidized bed reactor : Carbon and Sistema de recirculación acuícola con reactor de lecho fluidizado trifásico : Remoción de, *Revista Facultad de Ingeniería Universidad de Antioquia* 97 (2020): 93-102. <http://doi:10.17533/udea.redin.20200264..>
- [43] A. I. Alwared and W. Sh, Spiral path three phase fluidized bed reactor for treating wastewater contaminated with engine oil, *Appl. Water Sci.*, 10, 9 (2020) 1–11. <http://doi:10.1007/s13201-020-01290-4>.
- [44] F. Larachi, I. Iliuta, O. Rival, and B. P. A. Grandjean, Prediction of minimum fluidization velocity in three-phase fluidized-bed reactors, *Ind. Eng. Chem. Res.*, 39, 2 (2000) 563–572, <http://doi:10.1021/ie990435z>.
- [45] S. Sahoo, Fluidized bed reactor: design and application for abatement of fluoride, Bachelor of Technology ( Chemical Engineering ) (2012).
- [46] S. Ergun, Fluid Flow through Packed Columns, *Chem. Eng. Progress*, 48,2 (1952) 89–94.
- [47] R. K. Niven, Physical insight into the Ergun and Wen and Yu equations for fluid flow in packed and fluidised beds, *Chem. Eng. Sci.*, 57, 3 (2002) 527–534. [http://doi:10.1016/S0009-2509\(01\)00371-2](http://doi:10.1016/S0009-2509(01)00371-2).
- [48] Fortin Y, *Reacteurs a lit Fluidise Triphasique: Caracteristiques Hydrodynamiques et Melange des Particules Solides*, PhD thesis, Inst. Natl. Polytech. Lorraine, Lorraine, Fr. (1984).
- [49] Enrique Costa, Fluid Dynamics of Gas-Liquid-Solid Fluidized Beds, *Am. Chem. Soc.*, 25 (1986) 849–854. <http://doi.org/10.1021/i200035a002>.
- [50] G.H.Song, F. Bavarian, L.S.Fan, Hydrodynamics of three-phase fluidized bed containing cylindrical hydrotreating catalysts.,” *Can. J. Chem. Eng.*, 67,2 (1989) 265–275. <http://doi.org/10.1002/cjce.5450670213>.
- [51] S. Nacef, Hydrodynamique des lits fluidises gaz-liquide-solide, Ph.D. Dissertation, L’Institut National Polytechnique de Lorraine, (1991).
- [52] J.P.Zhang, N. Epstein, and J.R.Grace, Minimum fluidization velocities for gas-liquid-solid three-phase system. *Powder technology* 100.2-3 (1998): 113-118. [http://doi.org/10.1016/S0032-5910\(98\)00131-4](http://doi.org/10.1016/S0032-5910(98)00131-4).
- [53] K. Ramesh and T. Murugesan, Minimum fluidization velocity and gas holdup in gas – liquid – solid fluidized bed reactors, 136 (2002) 129–136. <http://doi:10.1002/jctb.533>.
- [54] R.S.Ruiz, F.Alonso, and J. Ancheyta, Minimum fluidization velocity and bed expansion characteristics of hydrotreating catalysts in ebullated-bed systems. *Energy & fuels* 18.4 (2004),1149-1155. <http://doi.org/10.1021/ef030184d>.
- [55] S. B. and C. L. Briens, Fluidization regimes in two- and three-phase fluidized beds: comparison between measurement techniques, *Can. J. Chem. Eng.*, 79 (2001) 430–437. <http://doi:10.1002/cjce.5450790316>.
- [56] H. A. Khawaja, Review of the phenomenon of fluidization and its numerical modelling techniques, 9, 4, (2015) 397–408. <http://doi:10.1260/1750-9548.9.4.397>.
- [57] G.B.Wallis, One-dimensional two-phase flow. McGraw-Hill, New York, (1969).
- [58] H.Li, Heat transfer and hydrodynamics in a three-phase slurry bubble column, Ph.D.Thesis of Philosophy, (1998).
- [59] J. Schweitzer, J. Bayle, and T. Gauthier, Local gas hold-up measurements in fluidized bed and slurry bubble column, *Chemical Engineering Science* 56.3 (2001): 1103-1110, [http://doi:10.1016/S0009-2509\(00\)00327-4](http://doi:10.1016/S0009-2509(00)00327-4).
- [60] F. Tao, S. Ning, B. Zhang, H. Jin and G. He, Simulation Study on Gas Holdup of Large and Small Bubbles in a High Pressure Gas-Liquid Bubble Column, *MDPI Process.*, 7 (2019) 594. <http://doi:10.3390/pr7090594>.
- [61] S. Sharaf, M. Zednikova, M. C. Ruzicka, and B. J. Azzopardi, Global and local hydrodynamics of bubble columns – Effect of gas distributor, *Chem. Eng. J.*, 288 (2016) 489–504. <http://doi:10.1016/j.cej.2015.11.106>.

- [62] A. A. Mouza, G. K. Dalakoglou, and S. V Paras, Effect of liquid properties on the performance of bubble column reactors with fine pore spargers, 60 (2005) 1465–1475. <http://doi:10.1016/j.ces.2004.10.013>.
- [63] V.K.Bhatia, and N. Epstein, Three-phase fluidization: A generalized wake model, Proc. Int. Conf. on Fluidization and Its Applications, Cepudues Editions, Toulouse, 380 (1974).
- [64] K.Ostergaard, Holdup, mass transfer, and mixing in three-phase fluidization, AIChE Symposium Series, 74(176) (1978) 82–86.
- [65] H.Yu, and B. E. Rittman, Predicting bed expansion and phase hold-up for three-phase fluidized bed reactors with and without biofilm, Water Res. 31(10) (1997) 2604–2616. [http://doi.org/10.1016/S0043-1354\(97\)00102-4](http://doi.org/10.1016/S0043-1354(97)00102-4).
- [66] H. M. Jena, G. K. Roy, and B. C. Meikap, Gas holdup in a three -phase fluidized bed with cylindrical particles, Natl. Conf. Front. Chem. Eng. (2007).
- [67] A. Catros, and J. R. Bernard Gas holdup above the bed surface and grid gas jet hydrodynamics for three phase fluidized beds, 63,5 (1985), 754-759. <http://doi.org/10.1002/cjce.5450630508>.
- [68] L.S.Fan, F.R. Bavarian, I.Gorowara, and B.E. Kreischer, Hydrodynamics of gas-liquid-solid fluidization under high gas hold-up conditions. Powder technology 53.3 (1987): 285-293. [http://doi.org/10.1016/0032-5910\(87\)80101-8](http://doi.org/10.1016/0032-5910(87)80101-8).
- [69] R.L.Gorowara, and L.S. Fan, Effect of surfactants on three-phase fluidized bed hydrodynamics., Industrial & engineering chemistry research 29.5 (1990): 882-891. <http://doi.org/10.1021/ie00101a025>.
- [70] Z.Chen, C.Zheng, and Y.Feng, Distributions of flow regimes and phase holdups in three-phase fluidised beds., Chemical engineering science 50.13 (1995): 2153-2159. [http://doi.org/10.1016/0009-2509\(95\)00004-0](http://doi.org/10.1016/0009-2509(95)00004-0).
- [71] M.Safoniuk,J.R. Grace, L.Hackman, and C.A Mcknight, Gas hold-up in a three-phase fluidized bed., AIChE J., 48,7 (2002), 1581 – 1587. <http://doi:10.1002/aic.690480720>.
- [72] G. V. Vinod, A.V., Ajeesh, and K.N., Reddy, Studies on gas hold-up in a Draft tube fluidised bed column., Indian Chem. Eng., 46 (2004) 229–23. <http://doi.org/10.1080/00194506.2010.485860>.
- [73] A. Bakopoulos, , Multi-phase fluidization in large-scale slurry jet loop bubble columns for methanol and or dimethyl ether production., Chemical engineering science 61.2 (2006): 538-557. <http://doi.org/10.1016/j.ces.2005.06.035>.
- [74] S. Nacef, S.Poncinb, A. Bouguettouchaa, and G. Wild, Drift flux concept in two- and three-phase reactors., Chemical engineering science, 62.24 (2007): 7530-7538. <http://doi.org/10.1016/j.ces.2007.08.031>.
- [75] S.M Son, S.H Kang, T.G Kang, P.S.Song, U.Y. Kim, Y. Kang, and H.K.Kang, Gas holdup and gas-liquid mass transfer in three-phase circulating fluidized-bed bioreactors. J. Ind. Eng. Chem., 13,1 (2007) 14-20.
- [76] M. H. Abdel-aziz, M. Z. El-Abd, and M. Bassyouni, Heat and mass transfer in three-phase fluidized bed containing high-density particles at high gas velocities, Int. J. Therm. Sci., 102 (2016) 145–153. <http://doi:10.1016/j.ijthermalsci.2015.11.020>.
- [77] E. N. Chiu, T.M. and Ziegler, Heat transfer in three- phase fluidized beds., AIChE journal., 29 (1983) 677-685. <https://doi.org/10.1002/aic.690290424>.
- [78] S. Kato, Y., Uchida, K., Kago, T. and Morooka, Liquid holdup and heat transfer coefficient between bed and wall in liquid-solid and gas-liquid-solid fluidized beds, Powder Technol., 28 (1981) 173–179. [http://doi.org/10.1016/0032-5910\(81\)87040-4](http://doi.org/10.1016/0032-5910(81)87040-4).
- [79] K. Muroyama, M. Fukuma and Yasunishi, Wall-to-bed heat transfer in liquid-solid and gas-liquid-solid fluidized beds, Part-II : Caned.J.Chem. Eng., 64 (1986),409-419. <http://doi.org/10.1002/cjce.5450640308>.
- [80] O. Nore, G. Wild, C. L. Briens, and A. Margaritis, Wall-to-bed heat transfer in three- phase fluidized beds of low density particles, Can J. of Chem. Eng., 72 (1994) 546-550. <http://doi.org/10.1002/cjce.5450720322>.
- [81] A. Zorana, and G. Radmila, Wall-to-bed heat transfer in vertical hydraulic transport and in particulate fluidized beds, International Journal of Heat and Mass Transfer, 51 (2008) 5942-5948. <http://doi.org/10.1016/j.ijheatmasstransfer.2008.03.030>.
- [82] B. Baker, and C.G.J., Armstrong, Heat transfer in three-phase fluidized beds, Powder Technol., 21 (1978) 195-204. [http://doi.org/10.1016/0032-5910\(78\)80089-8](http://doi.org/10.1016/0032-5910(78)80089-8).
- [83] A.R. Khan and J.F. Richardson, Heat transfer from plane surface to liquids and to liquid-solid fluidized beds, Chemical Engineering Journal., 38 (1983) 2053-2066. [http://doi.org/10.1016/0009-2509\(83\)80109-2](http://doi.org/10.1016/0009-2509(83)80109-2)
- [84] M. Magiliotou, Y.M. Chem, and L.S. Fan, Bed-immersed object heat transfer in a three- phase fluidized bed, AIChE J., 34 (1988) 1101-1106. <http://doi.org/10.1002/aic.690340620>.
- [85] X. Luo, P. Jiang, and L. Fan, High-pressure three-phase fluidization : hydrodynamics and heat transfer, AIChE J., 43 (1997) 2432–2445. <http://doi.org/10.1002/aic.690431007>.

- [86] K. Muroyama S. Okumichi Y. Goto Y. Yamamoto and S. Saito, Heat transfer from immersed vertical cylinders in gas-liquid and gas-liquid- solid fluidized beds, *Chemical Engineering and Technology*, 24 (2001) 835-842. [http://doi.org/10.1002/1521-4125\(200108\)24:8<835::AID-CEAT835>3.0.CO;2-9](http://doi.org/10.1002/1521-4125(200108)24:8<835::AID-CEAT835>3.0.CO;2-9).
- [87] J.R. Grace, and A. Stefanova, Heat transfer from immersed vertical tube in a fluidized bed of group A particles near the transition to the turbulent fluidization flow regime, *International Journal of Heat and Mass Transfer.*, 51 (2008),2020-2028. <http://doi:10.1016/j.ijheatmasstransfer.2007.06.005>
- [88] M. I. Abdul-wahab and S. A. Mohammed, Prediction of effective bed thermal conductivity and heat transfer coefficient in fluidized beds, *IJCPE Journal.* ,10 (2009) 1–8.
- [89] Y. Kang, I.S. Suh, and S.D. Kim, Heat transfer characteristics of three phase fluidized beds., *Chemical Engineering Communications* 34.1-6 (1985): 1-13. <http://doi:10.1080/00986448508911182>.
- [90] S. D. Kim, Y. Kang, and H. K. Kwon, Heat transfer characteristics in two- and three-phase slurry-fluidized beds, 32 (1986) 6–9. <http://doi.org/10.1002/aic.690320820>.
- [91] S. Kumar, and L.S.Iian, Heat transfer characteristics in viscous gas liquid and gas. liquid solid systems., *AIChE J.*, 40 (1994).
- [92] E. N. Chiu, and T.M. Ziegler, Liquid holdup and heat transfer coefficient in liquid-solid and three-phase fluidized beds, *AIChE J.*, 9 (1985) 1504–1509. <http://doi.org/10.1002/aic.690310913>.
- [93] Y. Hatate, S.Tajari, T. Fujita, T. Fukumoto, I. Hano, Heat transfer coefficient in three-phase vertical upflows of gas-liquid -fine solid particle particles system., *Journal of chemical engineering of Japan* 20.6 (1987): 568-574. <http://doi.org/10.1252/jcej.20.568>.
- [94] S. D. Kang. and Y. Kim, On the heat transfer mechanism in three phase fluidized beds., *Korean .I. Chem. Engng*, 5 (1988) 154-163. <http://doi:10.1007/BF02697670>.
- [95] S. D. Kim, Y. J. Lee, and J. O. Kim, Heat transfer and hydrodynamic studies on two- and three-phase fluidized beds of floating bubble breakers, *Experimental Thermal and Fluid Science* , (1988) 237–242. [http://doi.org/10.1016/0894-1777\(88\)90002-7](http://doi.org/10.1016/0894-1777(88)90002-7).
- [96] S. I. Kim J. O., Park., and D. H Kim, Heat transfer and wake characteristics in three-phase fluidized beds with floating bubble breakers, *Chemical Engineering and Processing: Process Intensification* 28.2 (1990): 113-119. [http://doi.org/10.1016/0255-2701\(90\)80007-R](http://doi.org/10.1016/0255-2701(90)80007-R)
- [97] Y. J. Cho, S. Jung, S. Hee, Y. Kang, and S. Done, Heat transfer and bubble properties in three-phase circulating fluidized beds, *Chemical engineering science* 56.21-22 (2001): 6107-6115. [http://doi.org/10.1016/S0009-2509\(01\)00256-1](http://doi.org/10.1016/S0009-2509(01)00256-1).
- [98] K. S. K. R. A. O. Patnaik, Heat transfer mechanisms in a gas - liquid-solid fluidized beds, *Proceedings of the World Congress on Engineering and Computer Science (WCECS 2007)*. 24-26,2007.
- [99] Z. Arsenijević, T. K. Radoičić, M. Đuriš, and Ž. Grbavčić, Experimental investigation of heat transfer in three- phase fluidized bed cooling column, *Chem. Ind. Chem. Eng. Q.*, 21, 4, (2015) 519–526. <http://doi: 10.2298/CICEQ141022008A>.
- [100] D. Ho, J. Hwa, H. Ryong, Y. Kang, H. Jung, and S. Done, Heat transfer in three-phase ( G / L / S ) circulating fluidized beds with low surface tension media, *Chem. Eng. Sci.*, 66, 14 (2011) 3145–3151. <http://doi: 10.1016/j.ces.2011.02.061>.
- [101] W.D. Deckwer, On the Mechanism of Heat Transfer in Bubble Column Reactors, *Chem. Eng. ScL*, 35 (1980) 1341-1346. [http://doi.org/10.1016/0009-2509\(80\)85127-X](http://doi.org/10.1016/0009-2509(80)85127-X).
- [102] A. Zaidi, B. Benchechou, M. Karioun, and A. Akharaz, Heat transfer in three-phase fluidized beds with Non-Newtonian pseudoplastic solutions, *Chem. Eng.*, 93 (1990) 135–146. <http://doi: 10.1080/00986449008911442>.
- [103] Y. C. Moharana, and M. K. Malik, Fluidization in conical bed and computational fluid dynamics (CFD) modeling of the bed, A Project submitted to the National Institute of Technology, Rourkela no., 108 (2008).
- [104] G. Q. Cao, M.Y. Liu, and J.P. Wen, Experimental measurement and numerical simulation for liquid flow velocity and local phase hold-ups in the riser of a GLSCFB, *Chemical Engineering and Processing: Process Intensification.*, 48(2009) 288-295. <http://doi.org/10.1016/j.cep.2008.04.004>.
- [105] S. S. R. Panneerselvam and G. D. Surender, CFD simulation of hydrodynamics of gas–liquid–solid fluidised bed reactor, *Chemical Engineering Science.*, 64 (2009) 1119-1135. <http://doi.org/10.1016/j.ces.2008.10.052>.
- [106] M. Hamidipour and J. Chen, CFD study on hydrodynamics in three-phase fluidized beds — Application of turbulence models and experimental validation, 78 (2012) 167–180. <http://doi: 10.1016/j.ces.2012.05.016>.
- [107] W. Li and W. Zhong, CFD simulation of hydrodynamics of gas-liquid-solid three-phase bubble column, *Powder Technol.*, *Powder Technology.*, 286 (2015) 766-788. <http://doi: 10.1016/j.powtec.2015.09.028>.

- [108] S.N. Saha, G.P. Dewangan, and R. Gadhewal Gas-Liquid-Solid Fluidized Bed Simulation by Computational Fluid Dynamics, *Int. J. Adv. Res. Chem. Sci.*, 3 (2016) 1–8. <http://doi.org/10.20431/2349-0403.0302001>.
- [109] Y. Liu, Numerical Simulation of Three-Phase Flows in the Inverse Fluidized bed, Scholarship @ Western, (2018).
- [110] P. Khongprom, W. Wanchan; K. Kamkham; and S. Limtrakul, CFD Simulation of the Hydrodynamics in Three Phase Fluidized Bed Reactor: Effect of Particle Properties, IEEE, (2020) <http://doi.org/10.1109/RI2C48728.2019.8999951>.
- [111] D. Z. Zhang, and W. B. Vanderheyden, The effects of mesoscale structures on the disperse two-phase flows and their closures for dilute suspensions. *Int. J. Multiphase Flows*, 28(5), (2002) 805–822. [http://doi.org/10.1016/S0301-9322\(02\)00005-8](http://doi.org/10.1016/S0301-9322(02)00005-8).